Part 1: Synthesis, Characterization, and Hydrolysis of Silicate Ester Prodrugs: Model Studies

Part 2: Amide Bond Formation Kinetics in the Selective Uptake of Aliphatic Amines in PEG-PLGA Block-Copolymer Nanoparticles

A Thesis

Submitted to the Faculty of the Graduate School

Of the University of Minnesota

By

Mallory Jo Richards

In Partial Fulfillment of the Requirements

For the Degree of

Masters of Science

Adviser: Professor Thomas R. Hoye

August 2011

University of Minnesota

Acknowledgments

I would first like to thank my adviser, Professor Tom Hoye, for the opportunity to work and learn in his laboratory over the past two years. I have appreciated his support and insight in decisions that I have made during my graduate career.

I would also like to acknowledge the many great chemists I was fortunate enough to work beside. Particularly those who have worked on the project with me: Professors Christopher Macosko and Jayanth Panyam, Jing Han, Kevin Pustulka, Andrew Michel, and Adam Wohl. I also very much appreciate the insights and lively discussions from by lab mates Brain Woods, Beeru Baire, Dr. Amanda Schmidt, and Susie Emond.

I want to acknowledge the University of Minnesota for funding through teaching assistantships, the Minnesota Futures Grant Program and the NIH (EB011671) for funding my research during the summer months.

I want to particularly thank my parents Roxanne and Joseph Richards for all the sacrifices they have made to put me through college and support through graduate school. Lastly, and most of all, I need to thank Jacob Schmidt for his unconditional support during the past two years. Without your love and support, I never would have got through this!

Abstract

The research presented in this thesis comprises two main projects: model studies for the synthesis, characterization and hydrolysis of silicate ester prodrugs, including a fluorescent model (Part 1), and amide bond formation kinetics to analyze the selective uptake of amines into polymer nanoparticles (Part 2). In Part 1 an array of trimenthoxy monoacyloxy orthosilicates were synthesized and the relative hydrolysis rates were measured. It was observed that extending the linear carbon chain on the acyloxy group changed the relative rate constants by less than an order of magnitude while adding more bulky side chains (isopropyl and *tert*- butyl) gave relative rate constants that stretched a full order of magnitude. I also outline the synthesis and fluorescence of a nitrobenzoxadiazole silicate ester and initial loading experiments of the fluorophore into polymer nanoparticles. In Part 2 I outline an experimental design that probes the selective uptake of amines to form amide bonds within PEG-PLGA nanoparticles. When two dialkylamines were competed a higher selectivity was observed for the more hydrophobic amine.

Table of Contents

List of Tables

List of Figures

1. Synthesis, Characterization, and Hydrolysis of Silicate Ester Prodrugs

1.1 Background.

As one of the leading causes of death in the United States, cancer is widely recognized as a foremost medical challenge to modern healthcare. Taxol® is a water-insoluble anti-cancer drug that was recognized in the 1990s as one of the most potent drugs among the approved anti-cancer drugs available. However the formulation for intravenous injection of Taxol® only contains *ca.* 1 wt% of its active agent paclitaxel.[1,2] The large amount of the surfactants, Cremophor® EL and ethanol, in this formulation leads to a wide range of undesirable side effects including heart arrhythmias, neutropenia (a decrease in white blood cells), complete alopecia (hair loss), and occasionally congestive heart failure.[3] Professors Thomas Hoye, Christopher Macosko, and Jayanth Panyam have formed a collaboration in an interest to develop improved formulations (targeted delivery, higher drug loading, etc) for the administration of paclitaxel by utilizing a hydrophobic-hydrophilic loaded block-copolymer (BCP) nanoparticles (NP) formed by flash nanoprecipitation (FNP).

Biodegradable polymeric nanoparticles are frequently used to improve the therapeutic value of various water insoluble drugs by improving bioavailability, solubility, and retention time.[4] These nanoparticle–drug formulations have the potential to reduce the patient expenses and risks of toxicity. Encapsulation of hydrophobic medicinal drugs allows for the increase in drug efficacy, specificity, tolerability, and therapeutic index.[5,6,7] These advantages are achieved because

these formulations protect the drug from premature degradation and interaction with the biological environment and allow for enhancement of absorption into a selected tissue, bioavailability, retention time, and improvement of intracellular penetration.

For improved targeting of our proposed formulation we are taking advantage of the enhanced permeation and retention (EPR) effect, which occurs when polymeric nanoparticles of the proper size (50-200nm) preferentially accumulate in a tumor tissue by passive targeting.[8,9,10] As seen in Figure 1, the vascular permeability of growing tumor tissues is enhanced, which allows for the increase in transport of macromolecules from the blood vessels to tumor tissues, while small molecules remain in the blood vessels. Furthermore, the lymphatic drainage system does not operate effectively in tumor tissues, resulting in macromolecules being selectively retained for an extended period of time in the growing tumor mass.[2] Taking advantage of this effect allows our polymer nanoparticles (100-200 nm) to be preferentially passed into the growing tumor tissue over small molecule administration of the drug.

Figure 1: The enhanced permeation and retention (EPR) effect.

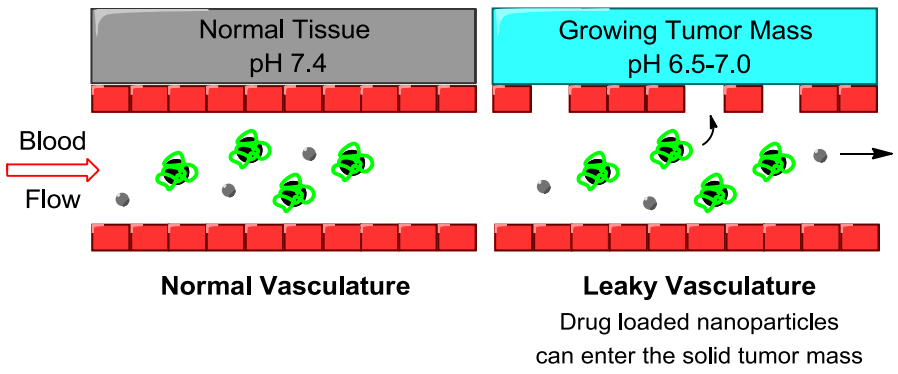

The formation of the BCP nanoparticles performed by FNP was first pioneered by Professor Prud'Homme et al. at Princeton University.[11] In FNP rapid co-precipitation of a hydrophilic-hydrophobic BCP and hydrophobic small molecules will form kinetically trapped morphologies rather than the more stable thermodynamically ordered micelles (Figure 2) that form through normal dialysis methods. Having the ability to kinetically trap the hydrophobic drug in the BCP leads to significantly increased loading ability of the drug, up to 80 wt%, for hydrophobic compounds such as β-carotene.

Figure 2: Flash nanoprecipitation (FNP).

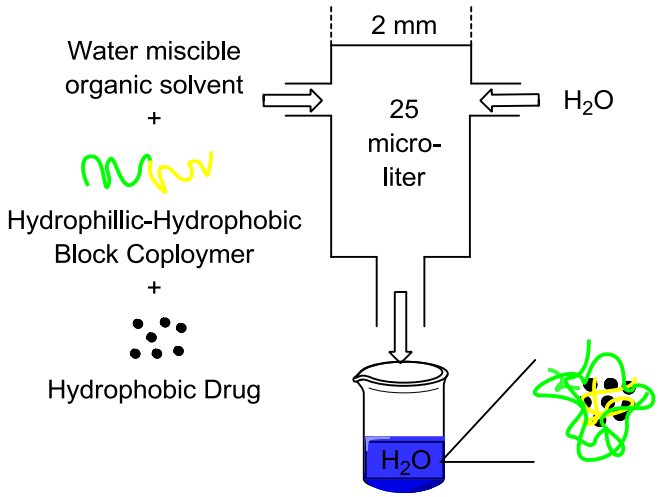

Previous efforts to encapsulate underivatized paclitaxel (**1**) into a biocompatible polyethylene glycol (PEG)-poly(lactic-coglycolic acid) (PLGA) BCP via FNP have failed to produce stable nanoparticles.[12] As earlier discovered in the Prud'Homme lab, Zengxi Zhu in the Hoye and Macosko groups observed that

rapid Ostwald ripening (<15 minutes) leads to the crystallization of **1** out of the BCP NPs.[13] Thus, paclitaxel is too hydrophobic to be dissolved in saline and administered directly as a drug solution, yet it is too hydrophilic to be effectively captured and stabilized in the hydrophobic NP core. Attempts to use hydrophobic ester derivatives of **1** gave considerably less bioactive (GI_{50} values) NPs, most likely because the esters were not cleaved efficiently to function as effective prodrugs.[14,15]

The use of silicate esters as prodrugs would dramatically increase the hydrophobicity of paclitaxel while at the same time giving it the ability to be easily hydrolyzed to its free active form. As a class, silicate esters are known to be reactive with water, hydrolyzing to orthosilicic acid [$Si(OH)_4$] and their corresponding alcohols (ROH). [16,17,18] Orthosilicic acid and its readily formed oligomeric homologs are commonly encountered in human biology, giving silicates the potential to be used as prodrugs with relatively little toxicity.[19] Previous silicate ester hydrolysis experiments have focused almost entirely on $Si(OMe)_4$ and $Si(OEt)_4$ and there are no evident applications of them in the field of bioactive medicinal agents nor, more specifically, of their use as prodrugs (Scheme 1) beyond the previous research preformed by the Professors' Hoye, Macosko, and Panyam research labs. [5,6,7]

Scheme 1: Formation of paclitaxel silicate ester.

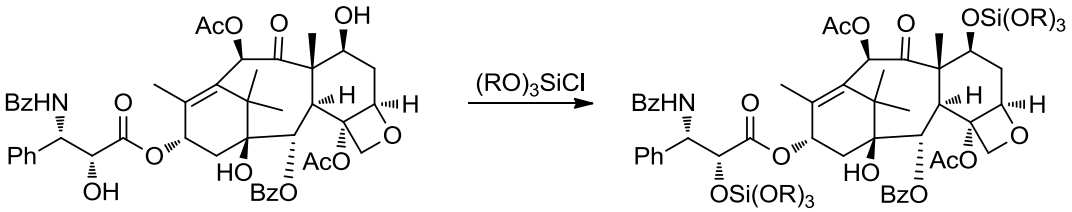

1 Paclitaxel

Paclitaxel Prodrug

Prior work performed in the Hoye group established trends of model silicate ester hydrolysis through ^{1}H NMR analysis. Through these studies it was established that significant changes in hydrophobicity (a longer hydrocarbon chain) showed less than an order of magnitude change in relative rate constants. However increased steric bulk (branching) of the aliphatic R group significantly decreased the relative rate of hydrolysis. Being able to fine tune the hydrolysis rates of the silicate esters over multiple orders of magnitude allows for the ability to control the desired release of paclitaxel from the paclitaxel prodrug in the more acidic tumor tissue.

1.2 Studies

1.2.1 Model Studies for Developing Hydrolysis Trends

Model studies were continued from previous work performed in the Hoye group to further explore the range of hydrolysis rates that can be achieved for the silicate esters. Previous studies performed by Adam Wohl and Yutaka Miura established a protocol to analyze the hydrolysis trends of the silicate esters by utilizing ^{1}H NMR spectroscopy. Other methods of analysis were examined (gas chromatography-mass spectrometry, and ^{29}Si NMR), however proton NMR was determined to be the most effective and convenient method that can be used on milligram scale. The method was established and preformed on symmetrical tetraalkoxy silicate esters in order to establish the trends stated in the background above.

For my contribution to understanding a variety of silicate ester hydrolysis rates, arrays of trimenthoxy monoacyloxy silicate esters were synthesized and the observed hydrolysis rates were measured by ^{1}H NMR spectroscopy (Scheme 2). These experiments were run in a 1:1:98 D_2O: TFA: Acetone-d_6 solvent ratio with trifluoroacetic acid (TFA) as the catalyst following the protocol previously established. To determine the observed hydrolysis rate the ratio of starting ester to free alcohol (particularly comparing the OC*H* integration value the silicate ester menthol to the free menthol formed upon hydrolysis) was plotted versus time and fit to an exponential function. The hydrolysis data showed that the addition of the

acyloxy group to the model silicate systems dramatically increased the rate of hydrolysis compared to the tetraalkoxy species (Table 1). It can be inferred that the rate determining step is the hydrolysis of the acyloxy species, particularly because no intermediate alkoxy silicate species were observed by ^{1}H NMR spectroscopy.

Scheme 2: Silicate ester hydrolysis rates.

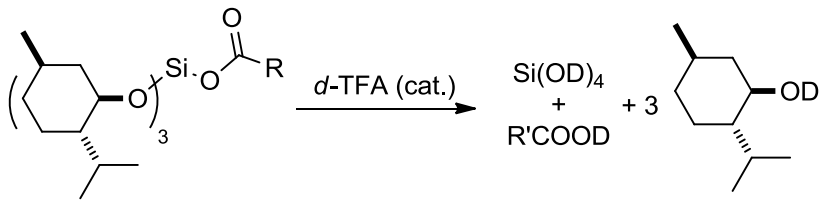

Table 1: Relative hydrolysis rates of model silicates.

Compound	R	D_2O : TFA: acetone-d_6 1:1:98 $k_{obs}(s^{-1})$	$t_{1/2}$ (min)
2	Methyl	$2.63 \pm 0.08 \times 10^{-4}$	44 ± 1
3	Ethyl	$1.99 \pm 0.06 \times 10^{-4}$	58 ± 2
4	*n*-Propyl	$1.18 \pm 0.05 \times 10^{-4}$	98 ± 4
5	*n*-Pentyl	$1.09 \pm 0.08 \times 10^{-4}$	106 ± 4
6	*i*-Propyl	$3.49 \pm 0.04 \times 10^{-5}$	331 ± 2
7	*t*-Butyl	$2.54 \pm 0.07 \times 10^{-5}$	455 ± 4

*It should be noted that the synthesis and hydrolysis of the compounds ***2*** and ***7*** were previously performed in the Hoye lab, the data listed above is my reproduction of that work.

1.2.2 Synthesis of Reactive Intermediates

To improve the synthetic pathways to various silicate esters key reactive intermediates (Figure 3) were synthesized and isolated. Our previous synthetic pathways involved one pot procedures (Scheme 3) where the order of addition and stoichiometry had to be carefully controlled. Even with controlled conditions often times numerous by-products would be present in the reaction mixtures, which had to be meticulously purified by medium-pressure liquid chromatography (MPLC). It should be noted that compound ***9*** has been synthesized and purified in the past, but to the best of my knowledge the shelf life and stability of the compound have never been determined.[20,21] Compound ***8*** was also synthesized previously were it was found to degrade when exposed to air after 2-3 weeks but again there was no data to indicate its stability under nitrogen and low temperatures as well as its stability on silica gel.[22] Having access to the reactive intermediates can also be beneficial if the compound being derivatized is very precious material, because it allows for the best reaction conditions without waste of material to by-products.

Figure 3: Key reactive intermediates

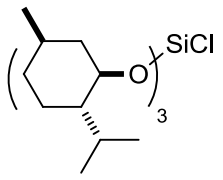

8

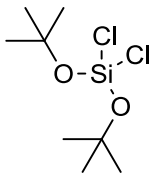

9

Scheme 3: One pot synthesis of silicate esters.

$$SiCl_4 + 3ROH \xrightarrow[2)\ R'COOH,\ Py]{1)\ Py,\ THF} (RO)_3SiOC(O)R'$$

The relative stability of the key intermediates was serendipitously discovered by a summer undergraduate student, Paul Alperin, who collected compound ***8*** from his MPLC column. From that observation efforts were made to synthesize and purify the above reactive intermediates on larger scales. Having the ability to make and store (in freezer) these compounds allows for efficient syntheses of future compounds.

Depending on the various properties of each reactive intermediate, it was either purified by a high vacuum distillation, ***9***, or by MPLC, ***8***, after which either of the compounds can be stored under nitrogen in the freezer for many weeks, 4-8, without degradation.

1.2.3 Fluorescent Silicate Model

It has been shown that drug release from PEG-PLGA BCP nanoparticles can be monitored by ultra violet-visible (UV-VIS) and fluorescent spectroscopy.[23,24,25] To explore characteristics of our silicate ester loaded BCP NPs and for a potential new way to monitor hydrolysis rates the fluorescent silicate model ***12*** was synthesized (Scheme 4). The fluorescence in this model originates from the nitrobenzoxadiazole (NBD) moiety of the silicate ester. The

reason for selecting the NBD moiety as our fluorophore comes from the ease of our ability to synthetically manipulate ***10*** to give free alcohol ***11*** attached to the NBD which would allow for efficient silicate ester formation. Also the triisopropyl monochloro silane as the model silicate was chosen for ease of synthesis, difficulty in utilizing trimenthoxy moiety, and stability (e.g., the triethoxy moiety degraded/hydrolyzed too quickly).

Scheme 4: Synthesis of silicate fluorophores.

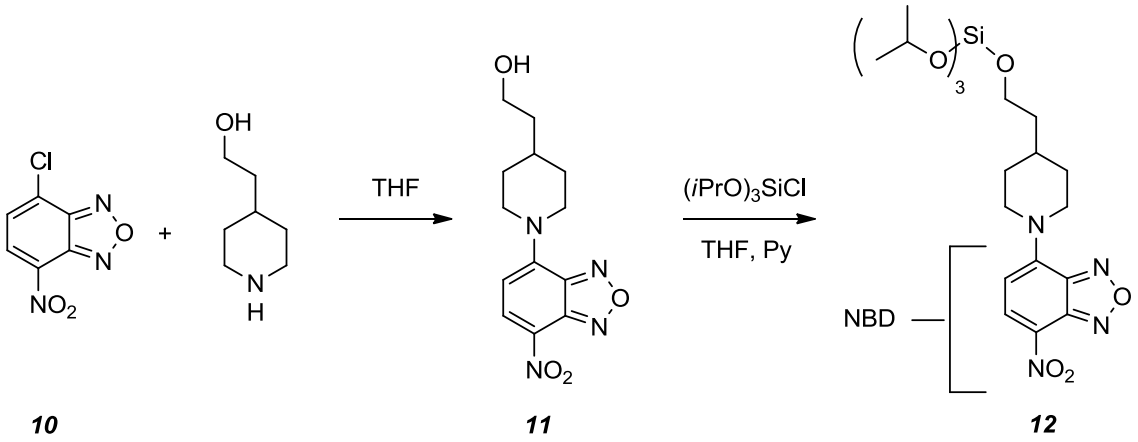

10 ***11*** ***12***

The fluorescence of ***12*** was measured using a PTI Quantamaster Fluorimeter in a range of solvents at the same concentration (Figure 4). The fluorescence data indicated that that there is a solvent dependency that can significantly affect the quantum yields (absorbance) of the fluorophore but minimally changes the emission wavelength. It was observed that the more polar the solvent the lower the absorptivity in the case of alcohol ***12.***[26] From this result it could be inferred that the dramatic difference in absorbance between water and ethanol and the other solvents could also be an effect of solvation. Even though measures were taken to ensure the compound was completely dissolved at such

minimal concentrations it is difficult to state directly whether it was completely dissolved or not.

Figure 4: Fluorescence of ***11*** in various solvents at 9.375 x 10^{-7} M.

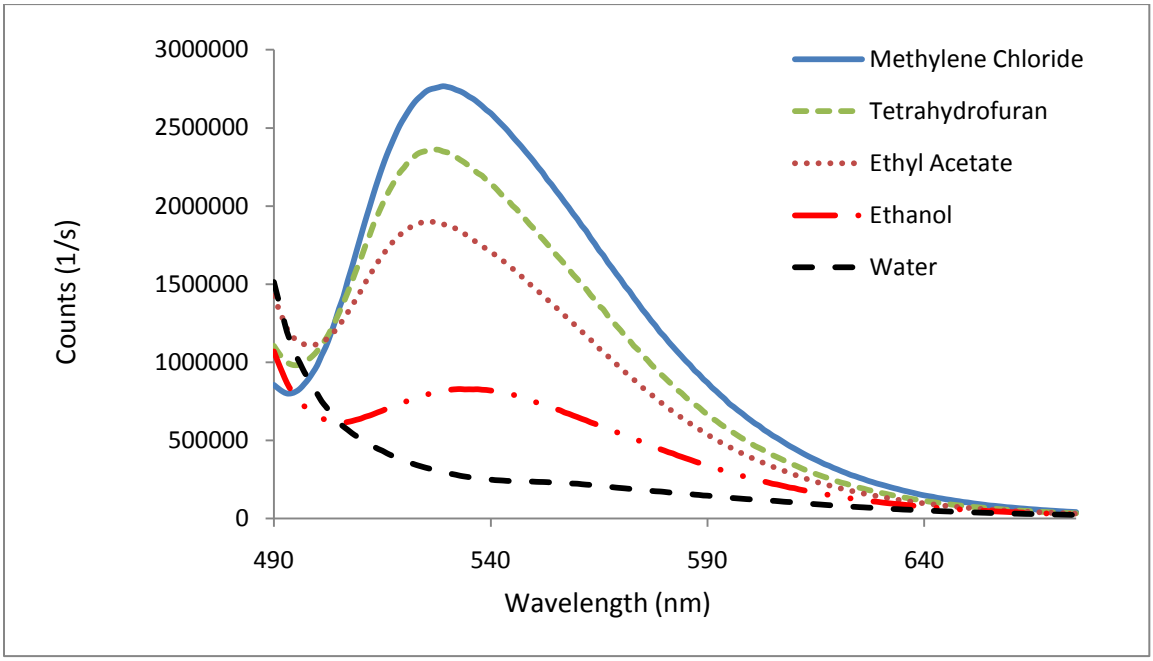

For the case of compound ***12*** ,the silicate ester, the inverse trend was observed (Figure 5). The greater the polarity the higher the absorptivity and in this case no absorbance was observed for either ethanol or water. It is expected that compound ***12*** is even less soluble in those solvents due to the very hydrophobic silicate ester now attached.

Figure 5: Fluorescence of ***12*** in various solvents at 5.8541 x 10^{-7} M

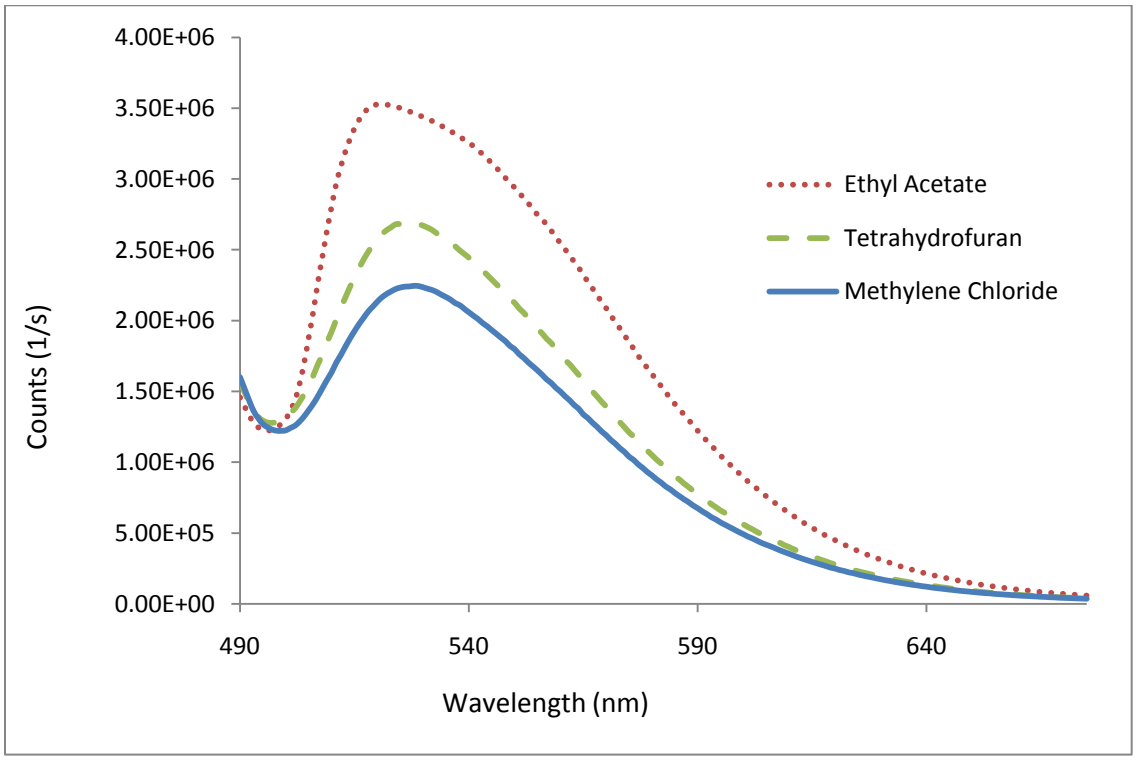

The fluorescence spectra of ***12*** loaded into PEG-PLGA (5K - 10K, respectively) BCP NPs formed by FNP were taken to test whether fluorescence could be detected in the hydrophobic nanoparticle core (Figure 6). A control was done where ***12*** was run through the flash nanoprecipitation protocol without the polymer present. In that case little to no fluorescence was observed and after a few minutes a red precipitate of the fluorophore formed in the suspension. From this observation it was determined that the ability to detect the fluorescence may be a solubility concern where ***12*** is soluble in the hydrophobic PLGA core but insoluble in the 95:5 H_2O: THF solvent ratio on the outside of the NPs. An absorbance decrease over time of the loaded NPs was also observed. There could be multiple reasons to explain this phenomenon (the fluorophore is being

released from the core of the NP, the environment around the fluorophore is changing, etc) and more testing would have to be done to determine the precise cause.

Figure 6: Fluorescence of BCP FNP NPs loaded with ***12*** in a 95:5 H_2O: THF solvent ratio.

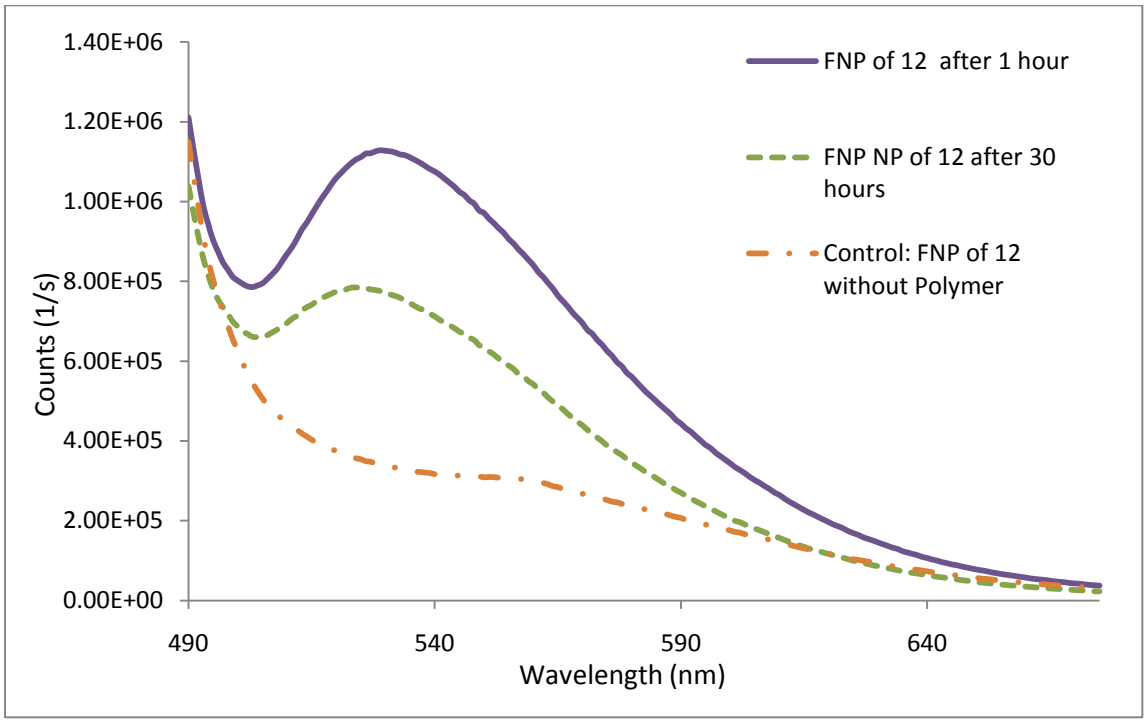

In order to learn more about the loading capacity of the silicate fluorophore, an array of nanoparticles were prepared with a loading level varying from 0.1 mg to 3.0 mg of ***12*** (Figure 7). From these data a few interesting observations can be taken. The first is that as the loading level increases there is a red shift in the wavelength. Red shifts can happen when there is a decrease in the energy between the ground and excited state, which often occurs when there is a change in the environment (often polarity) surrounding the fluorophore.[27]

This characteristic red shift of the fluorescence in a polymeric environment has precedent in literature with BCP micelles loaded with PRODAN (6-propionyl-2-(*N,N*-dimethylamino)naphthalene), a hydrophobic fluorophore.[28] Where PRODAN displays a 50 nm red shift in the nanoparticle and, in comparison, our silicate fluorophore experiences *ca.* a 40 nm shift. In this new polymeric environment more of ***12*** may be soluble (and/or loaded) than in the smaller nanoparticles (50-200 nm) that are initially formed by FNP.

For increase in the concentration of ***12*** in the NP suspension (going from 0.1 mg to 3.0 mg) the fluorescence appeared to decrease. (It should be noted that the fluorescence of the 0.1 mg loaded NP suspension had to be diluted even more than the otherwise standard concentration (1.86×10^{-6} M) of the fluorophore because it was initially off scale). This was an interesting phenomenon that again may be attributed to solvation effects. At the higher loading levels it is shown that a different environment may be forming (red shift) around the silicate ester fluorophore, which may be portraying a change from nanoparticles to larger ordered micelles. This is possibly occurring because 3.0 mg of hydrophobic silicate ester fluorophore loading is too concentrated to form the kinetically trapped nanoparticles usually seen by FNP and that when the nanoparticles fail to form, the thermodynamically favored larger micelles could be created.

Figure 7: Fluorescence of ***12*** at different loading levels in BCP NP.

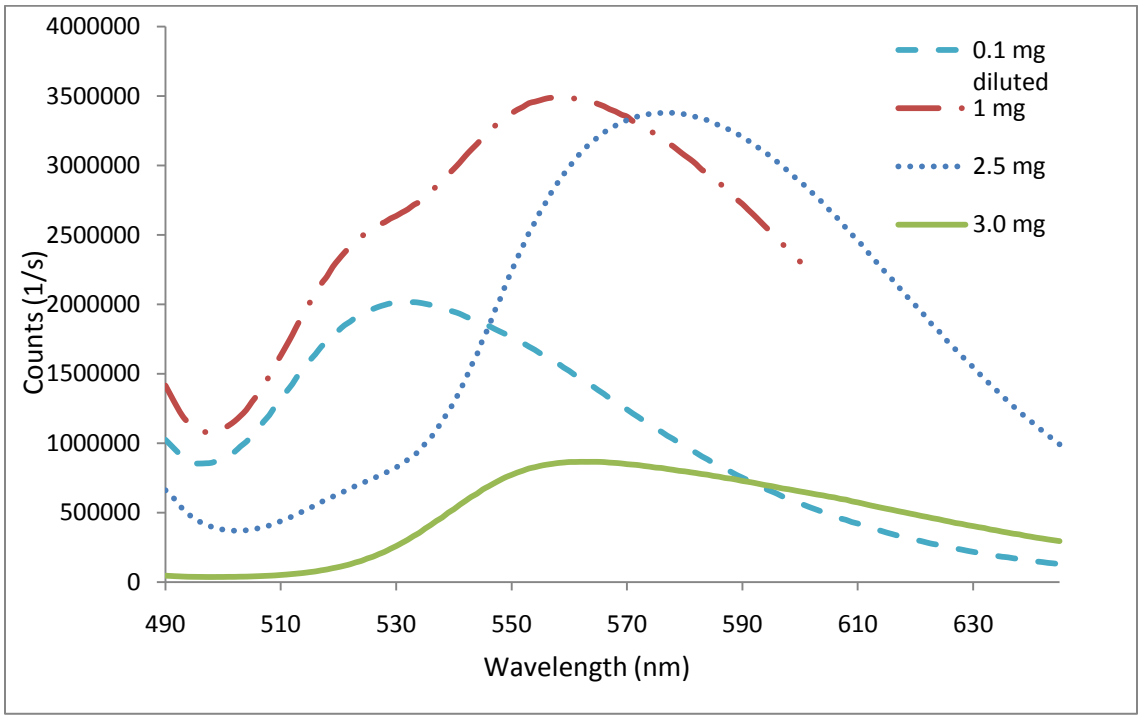

Due to the unusual nature of the higher concentrations of the fluorophore having lower absorptivities, the 3.0 mg loaded nanoparticle was monitored over time (Figure 8). It was shown that quickly (~20 min) the absorbance increased dramatically to the levels of the NP formulations with the lower wt% of fluorophore.

Figure 8: Fluorescence monitoring of 3.0 mg of ***12*** in BCP Nanoparticles.

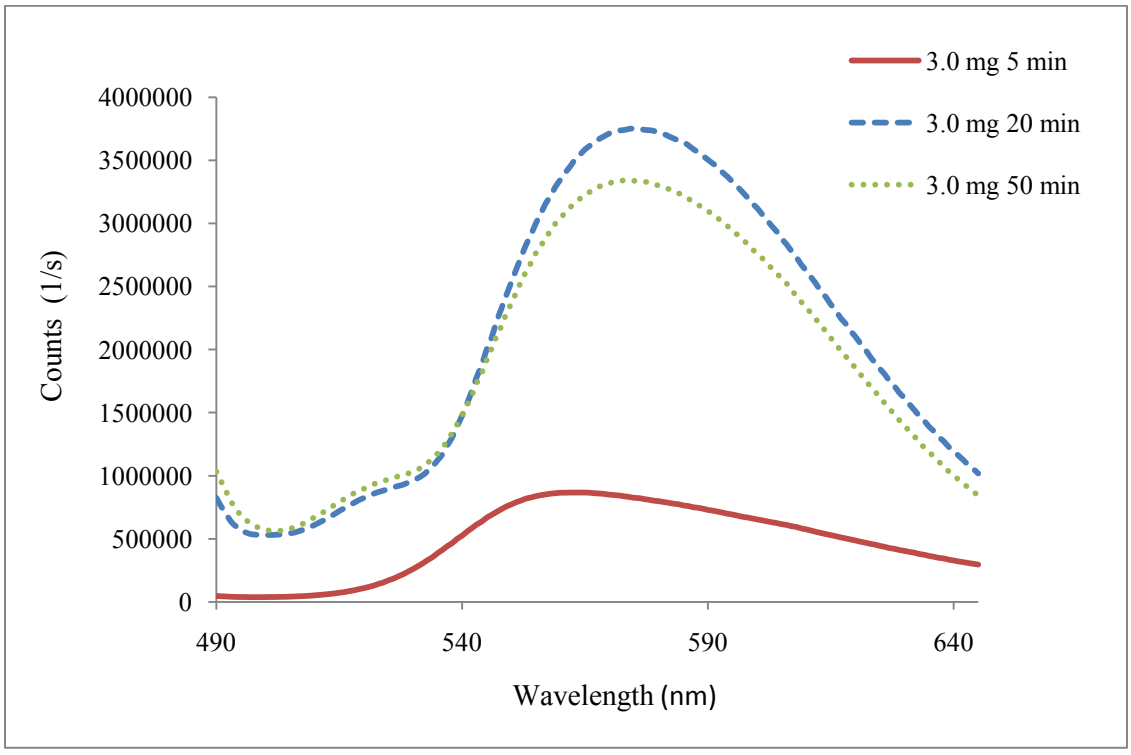

1.3 Conclusions

An array of trimenthoxy monoacyloxy silicate esters was synthesized and purified to test their rates of hydrolysis. From those experiments it was determined that extending the linear carbon acyloxy side chain altered the observed rate constant by less than an order of magnitude. However, the addition of steric bulk (branching) on the acyloxy side chain did give an order of magnitude difference. In general the addition of the acyloxy group versus an

alkoxy group (pervious work performed in the Hoye lab) significantly increases the rate of hydrolysis.

Key reactive intermediates were synthesized and isolated on a gram scale. These intermediates allow for the easy synthesis of future silicate esters and for increased yields due to the lack of by-product formation that happens in a one pot synthesis. It was also determined that these reactive intermediates could be stored in nitrogen in a freezer for several weeks with no degradation.

A fluorescent triisopropyl silicate ester model was synthesized using the nitrobenzoxadiazole moiety to provide fluorescence. The model showed an absorbance that depended on the solvent polarity, but it can also be inferred that the very hydrophobic nature of the silicate ester provided solubility issues in such solvents like water and ethanol. A few notable observations include a decrease in absorption of the silicate loaded into BCP NPs over time, a significant red shift in the wavelength of the silicate ester loaded into the nanoparticles, and variability in the fluorescent absorption and wavelength at various wt% load levels of the silicate fluorophore in the NPs. Hypotheses were made to explain these observations; however, more experiments and results are needed to make more substantial claims.

1.4 Experimental

All reactions requiring anhydrous conditions were carried out in oven-dried glassware under a nitrogen atmosphere. Anhydrous dichloromethane and tetrahydrofuran were obtained by passage through a column of activated alumina, and pyridine was distilled from calcium hydride.

All chemicals, unless otherwise noted, were purchased from Acros Chemical Company, Aldrich Chemical Company, and MP Biomedicals. ^{1}H and ^{13}C NMR spectra were run on a 500 MHz or 300 MHz Varian Inova spectrometer, chemical shifts are referenced to TMS (0.0 ppm) for spectra collected in $CDCl_3$ and to acetone (2.05 ppm) for spectra collected in $CO(CD_3)_2$. The fluorescence date was collected on a Quantamaster Fluorimeter with the excitation wavelength set at 475 nm (λ_{max} in UV-Vis spectrum).

1.4.1 Hydrolysis Experiments

All of the hydrolysis experiments performed on the monoacyloxy trimenthoxy silicates were done in 98:1:1 acetone-d_6: D_2O:TFA solvent mixture. As soon as the TFA was added to the solution time points were taken frequently ranging from 30 minutes to a few hours depending on the substrate. All the hydrolysis experiments were done in triplicate. To achieve the observed rate constants the ratio of starting material to hydrolyzed product was plotted vs time. The relative amount of the starting material and product was determined by ^{1}H NMR spectroscopy in particular measuring the –OC*H* peak in the starting material and product. An example excel plot of the ratios over time is shown below for monoacetoxy trimenthoxy orthosilicate.

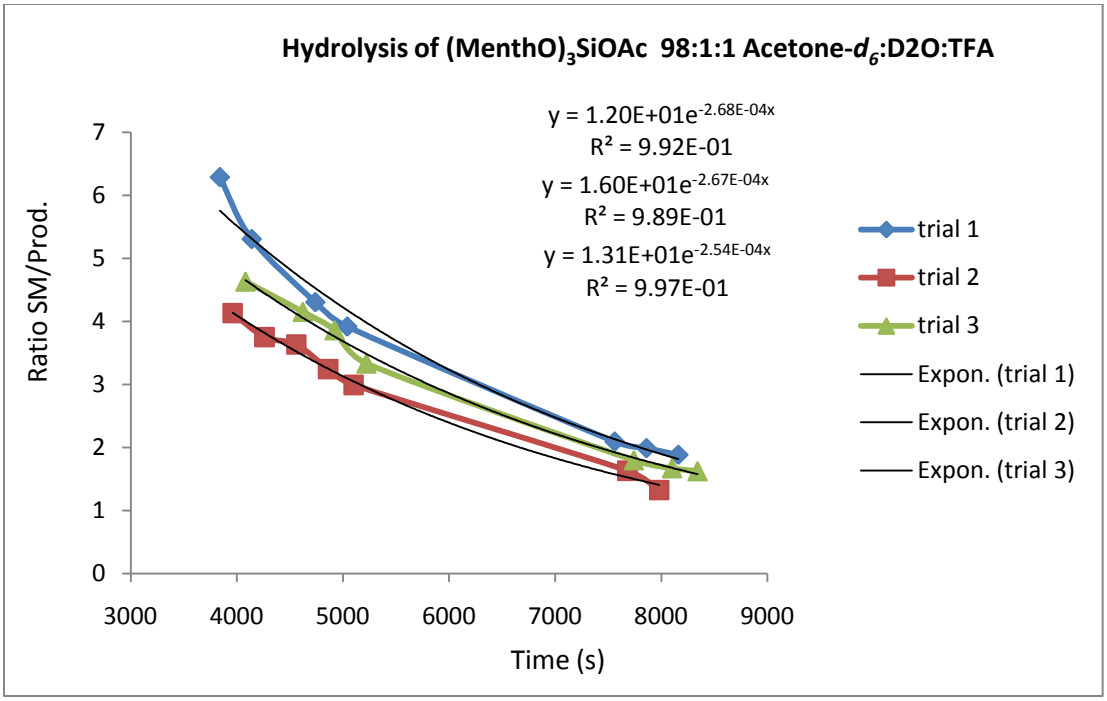

1.4.2 Synthetic Work

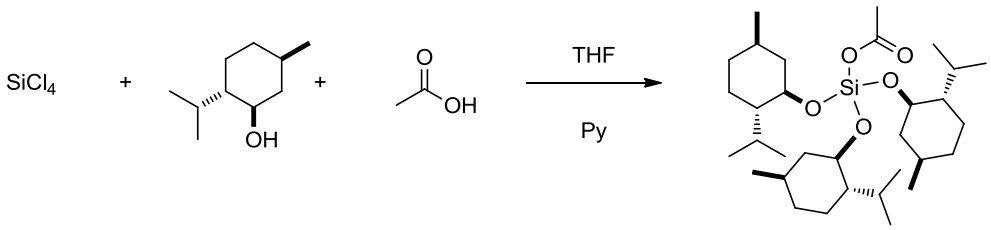

Acetic ((tris(1R,2S,5R)-2-isopropyl-5-methylcyclohexyl) orthosilicic) anhydride (*2*). THF (200 mL) was placed in a 250 mL round bottom flask, placed under a nitrogen atmosphere, and stirred. $SiCl_4$ (0.5 ml, 4.36 mmol) was added by glass syringe. Menthol (2.078 g, 13.3 mmol), pyridine (0.344 g, 13.3 mmol), and THF (20 mL) were combined and added dropwise to the $SiCl_4$ mixture. After

1 h acetic acid (0.2618 g, 4.36mmol) and pyridine (0.3441 g, 4.36 mmol) were added by syringe to the reaction mixture. The reaction was monitored by TLC (95:5, hexanes: ethyl acetate). After 4 h the mixture was filtered, concentrated, and purified by MPLC (98:2, hexanes: ethyl acetate) to yield a clear colorless oil (40%). **^{1}H NMR** (500 MHz, C(O)D_6): δ 3.80 (dt, *J* = 10.3, 3.9 Hz, 3H, SiOC*H*), 2.07 (s, 3H, COC*H*$_3$), 2.28 (dsept, *J* = 2.5, 6.9 Hz, 3H, $(CH_3)_2$C*H*), 2.11 (m, 3H, SiOCHCH_A*H*$_E$), 1.63 (m, 6H, $(CH_3)_2$CHCHCH_A*H*$_E$CH_A*H*$_E$), 1.39 (m, 3H, CH_3C*H*), 1.18 (ddt, *J* = 3.0, 9.8, 10.3 Hz, 3H, $(CH_3)_2$CHC*H*), 1.03 (app. q, *J* = 12.2 Hz, 3H, $(CH_3)_2$CHCHC*H*$_A$H$_E$), 0.92 (m, 3H, $(CH_3)_2$CHCHCH_2C*H*$_A$H$_E$), 0.90 (dd, *J* = 1.5, 6.5 Hz, 18H, (C*H*$_3$)$_2$), 0.85 (m, 3H, SiOCHC*H*$_A$H$_E$), and 0.79 (d, *J* = 6.9 Hz, 9H, C*H*$_3$); **^{13}C NMR:** (125 MHz, CO$(CD_3)_2$) 212.11, 76.56, 68.36, 51.30, 45.99, 35.74, 32.92, 26.38, 23.97, 23.41, 22.32, and 16.72; **HR ESI-MS**: calcd for $C_{32}H_{60}NaO_5Si$ 575.4102[M + Na]$^+$, found 575.4102; **IR** (CH_2Cl_2): 2953, 2910, 2848, 1738, 1457, 1383, 1369, 1246, 1237, 1179, 1084, 1051, and 1002 cm^{-1}.

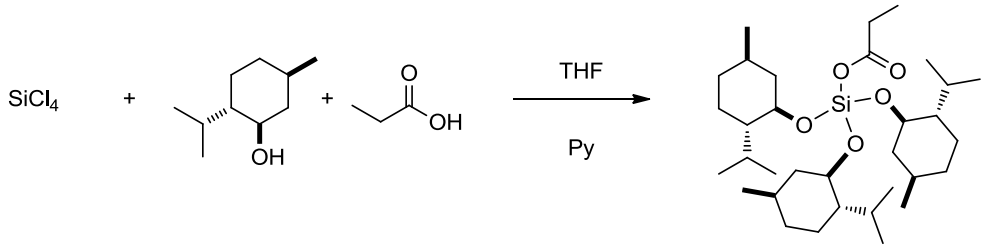

Propionic (tris((1R,2S,5R)-2-isopropyl-5-methylcyclohexyl) orthosilicic) anhydride (*3*) . THF (100 mL) was placed in a 250 mL round bottom flask, placed under a nitrogen atmosphere, and stirred. $SiCl_4$ (0.5 ml, 4.36 mmol) was added by glass syringe. Menthol (2.078 g, 13.3 mmol), pyridine (0.344 g, 13.3

mmol), and THF (20 mL) were combined and added dropwise to the $SiCl_4$ mixture. After 1 h propionic acid (0.3230 g, 4.36mmol) and pyridine (0.3449 g, 4.36 mmol) were added by syringe to the reaction mixture. The reaction was monitored by TLC (95:5, Hexane: Ethyl Acetate). After 4 h the mixture was filtered, concentrated, and purified by MPLC (99:1, Hexanes: Ethyl Acetate) to yield a crystalline white solid. **^{1}H NMR** (500 MHz, $CO(CD_3)_2$): δ 3.82 (dt, *J* = 4.4, 10.3 Hz, 3H, SiOC*H*), 2.38 (q, *J* = 7.8 Hz, 2H, COCH_2), 2.28 (dsept, *J* = 3.0, 7.3 Hz, 3H, $(CH_3)_2$C*H*), 2.11 (m, 3H, SiOCHC$H_A$$H_E$), 1.63 (m, 6H, $(CH_3)_2$CHCHC$H_A$$H_ECH_A$$H_E$), 1.39 (m, 3H, CH_3C*H*), 1.18 (tt, *J* = 2.9, 8.3 Hz, 3H, $(CH_3)_2$CHC*H*), 1.10 (t, *J* = 7.4 Hz, 3H, $COCH_2CH_3$), 1.04 (app. q, *J* = 12.2 Hz, 3H, $(CH_3)_2$CHCHC$H_A$$H_E$), 0.96 (m, 3H, $(CH_3)_2$CHCHCH_2C$H_A$$H_E$), 0.90 (dd, *J* = 6.4, 7.4 Hz, 18H, (CH_3)$_2$), 0.85 (m, 3H, SiOCHC$H_A$$H_E$), and 0.75-0.73 (d, *J* = 6.9 Hz, 9H, CH_3); **^{13}C NMR:** (125 MHz, $CO(CD_3)_2$) 215.12, 74.69, 50.79, 45.51, 35.21, 32.42, 26.04, 23.47, 22.63, and 21.63; **HR ESI-MS**: calcd for $C_{33}H_{62}NaO_5Si$ 589.4259$[M + Na]^+$, found 589.4252; **IR** (CH_2Cl_2): 2949, 2866, 2722, 1732, 1455, 1419, 1384, 1368, 1348, 1324, 1280, 1235, 1180, 1151, 1083, and 1002 cm^{-1}.

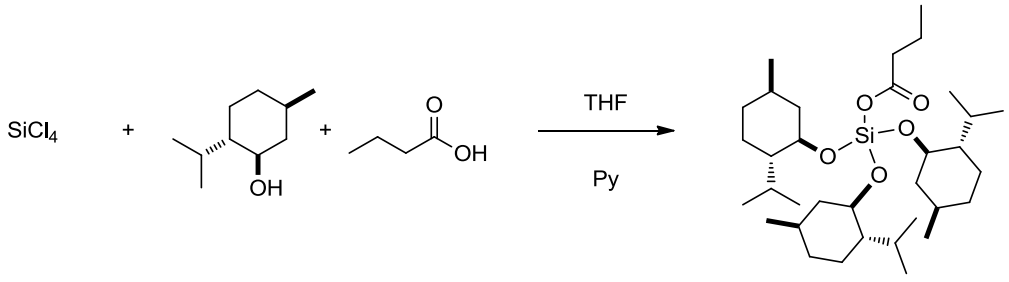

Butyric(Tris(1R,2S,5R)-2-isopropyl-5-methylcyclohexyl)orthosilicic) anhydride (*4*). THF (175 mL) was placed in a 250 mL round bottom flask, placed under a nitrogen atmosphere, and stirred. $SiCl_4$ (0.5 ml, 4.36 mmol) was added by glass syringe. Menthol (2.078 g, 13.3 mmol), pyridine (0.344 g, 13.3 mmol), and THF (20 mL) were combined and added dropwise to the $SiCl_4$ mixture. After 1 h butyric acid (0.3449 g, 4.36mmol) and pyridine (0.3449 g, 4.36 mmol) were added by syringe to the reaction mixture. The reaction was monitored by TLC (95:5, Hexanes: Ethyl Acetate). After 4 h the mixture was filtered, concentrated, and purified by MPLC (99.5:0.5, Hexanes: Ethyl Acetate) to yield a clear colorless oil. **^{1}H NMR** (500 MHz, $CDCl_3$): δ 3.76 (dt, *J* = 10.8, 4.4 Hz, 3H, SiOC*H*), 2.33 (t, *J* = 7.3 Hz, 2H, COCH_2), 2.23 (dsept, *J* = 2.5, 6.9 Hz, 3H, $(CH_3)_2CH$), 2.05 (m, 3H, $SiOCHCH_AH_E$), 1.63 (p, *J* = 7.4 Hz, 2H, $C(O)CH_2CH_2$), 1.60 (m, 6H, $(CH_3)_2CHCHCH_AH_ECH_AH_E$), 1.36 (m, 3H, CH_3CH), 1.19 (tt, *J* = 2.9, 5.6 Hz, 3H, $(CH_3)_2CHCH$), 1.05 (app. q, *J* = 12.2 Hz, 3H, $(CH_3)_2CHCHCH_AH_E$), 0.96 (t, *J* = 7.4 Hz, 3H, $COCH_2CH_3$), 0.93 (m, 3H, $(CH_3)_2CHCHCH_2CH_AH_E$), 0.89 (app. t, *J* = 6.4, Hz, 18H, $(CH_3)_2$), 0.84 (m, 3H, $SiOCHCH_AH_E$), and 0.75 (d, *J* = 6.8 Hz, 9H, CH_3); **^{13}C NMR:** (125 MHz,$CDCl_3$) 73.97, 49.61, 44.46, 37.69, 34.40, 31.58, 25.19, 22.66, 22.20, 21.18, 18.33, 15.66, 14.13, and 13.61; **HR ESI-MS**: calcd for $C_{34}H_{64}NaO_5Si$ 603.4415$[M + Na]^+$, found 603.4426; **IR** (film): 3055, 2986, 2957, 2927, 2871, 2306, 1718, 1703, 1456, 1371, and 1180 cm^{-1}.

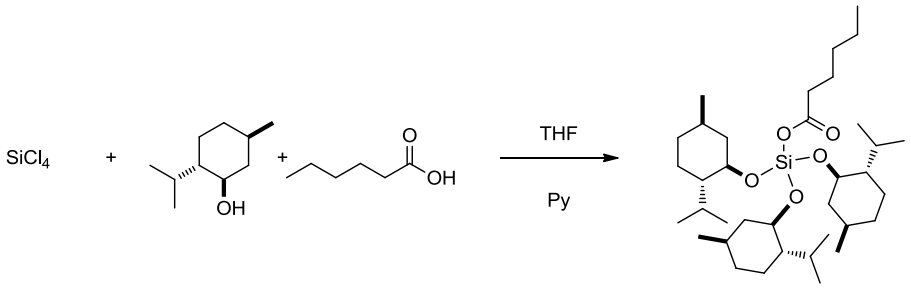

Hexanoic (tris((1R,2S,5R)-2-isopropyl-5-methylcyclohexyl) orthosilicic) anhydride (*5*). THF (200 mL) was placed in a 250 mL round bottom flask, placed under a nitrogen atmosphere, and stirred. $SiCl_4$ (0.5 ml, 4.36 mmol) was added by glass syringe. Menthol (2.078 g, 13.3 mmol), pyridine (0.344 g, 13.3 mmol), and THF (20 mL) were combined and added dropwise to the $SiCl_4$ mixture. After 1 h hexanoic acid (0.5065 g, 4.36mmol) and pyridine (0.3441 g, 4.36 mmol) were added by syringe to the reaction mixture. The reaction was monitored by TLC (95:5, Hexane: Ethyl Acetate). After 4 h the mixture was filtered, concentrated, and purified by MPLC (99.5: 0.5, Hexanes: Ethyl Acetate) to yield a clear colorless oil. **^{1}H NMR** (500 MHz, $CDCl_3$): δ 3.77 (dt, *J* = 10.3, 4.4 Hz, 3H, SiOC*H*),2.33 (t, *J* = 7.3 Hz, 2H, C(O)CH_2), 2.23 (dsept, *J* = 2.0, 6.9 Hz, 3H, $(CH_3)_2CH$), 2.05 (m, 3H, SiOCHC$H_A H_E$), 1.72 (m, 2H, C(O)CH_2CH_2), 1.60 (m, 6H, $(CH_3)_2$CHCHC$H_A H_E$C$H_A H_E$), 1.36 (m, 3H, CH_3CH),1.31 (m, 7H, C(O)CH_2CH_2CH_2CH_2CH_3), 1.30 (m, 3H, $(CH_3)_2$CHC*H*), 1.20 (m, 6H, C(O)CH(CH_3)$_2$), 1.06 (m, 3H, $(CH_3)_2$CHCHCH_AH$_E$), 0.95 (m, 3H, $(CH_3)_2$CHCHCH$_2$CH_AH$_E$), 0.89 (dd, *J* = 5.6, 5.6 Hz, 18H, (CH_3)$_2$), 0.84 (m, 3H, SiOCHCH_AH$_E$), and 0.75 (d, *J* = 7.3 Hz, 9H, CH_3); **^{13}C NMR:** (125 MHz,$CDCl_3$) 73.97, 49.62, 44.46, 35.87, 34.40, 31.59, 31.27, 25.20, 24.68, 22.66, 22.41, 22.20, 21.18, 15.68, 14.12, and 13.92; **HR ESI-MS**: calcd for $C_{36}H_{68}NaO_5Si$

631.4728[M + Na]$^+$, found 631.4729; **IR** (thin film): 3055, 2984, 2957, 2927, 2871, 2306, 1716, 1703, 1456, 1368, and 1180 cm^{-1}.

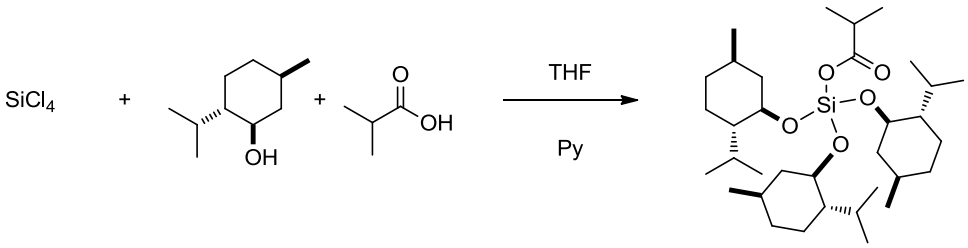

Isobutyric(tris((1R,2S,5R)-2-isopropyl-5-methylcyclohexyl) orthosilicic) anhydride (*6*). THF (200 mL) was placed in a 250 mL round bottom flask, placed under a nitrogen atmosphere, and stirred. $SiCl_4$ (0.5 ml, 4.36 mmol) was added by glass syringe. Menthol (2.078 g, 13.3 mmol), pyridine (0.344 g, 13.3 mmol), and THF (20 mL) were combined and added dropwise to the $SiCl_4$ mixture. After 1 h isobutyric acid (0.3842 g, 4.36mmol) and pyridine (0.3441 g, 4.36 mmol) were added by syringe to the reaction mixture. The reaction was monitored by TLC (95:5, Hexane: Ethyl Acetate). After 4 h the mixture was filtered, concentrated, and purified by MPLC (99.5:0.5, Hexanes: Ethyl Acetate) to yield a clear colorless oil. **^{1}H NMR** (500 MHz, $CDCl_3$): δ 3.76 (dt, *J* = 10.3, 3.9 Hz, 3H, SiOC*H*), 2.55 (sep, *J* = 6.9 Hz, 1H, C(O)C*H*$(CH_3)_2$), 2.23 (dsept, *J* = 2.5, 7.1 Hz, 3H, $(CH_3)_2$C*H*), 2.05 (m, 3H, SiOCHCH_A*H*$_E$), 1.72 (m, 2H, C(O)CH_2C*H*$_2$), 1.61 (m, 6H, $(CH_3)_2$CHCHCH_A*H*$_E$CH_A*H*$_E$), 1.36 (m, 3H, CH_3C*H*), 1.29 (m, 3H, $(CH_3)_2$CHC*H*), 1.17 (d, *J* = 6.9 Hz, 6H, C(O)CH(C*H*$_3$)$_2$), 1.05 (app. q, *J* = 12.2 Hz, 3H, $(CH_3)_2$CHCHC*H*$_A$H$_E$), 0.95 (m, 3H, $(CH_3)_2$CHCHCH_2C*H*$_A$H$_E$), 0.89 (app. t, *J* = 5.6, Hz, 18H, (C*H*$_3$)$_2$), 0.84 (m, 3H, SiOCHC*H*$_A$H$_E$), and 0.75 (d, *J* = 6.8 Hz, 9H,

C*H*$_3$); **^{13}C NMR:** (125 MHz,$CDCl_3$) 73.98, 49.61, 44.49, 34.42, 31.59, 25.23, 22.72, 22.21, 21.18, 18.88, 15.73, and 14.13; **HR ESI-MS**: calcd for $C_{34}H_{64}NaO_5Si$ 603.4415[M + Na]$^+$, found 603.4452; **IR** (thin film): 3055, 2984, 2957, 2927, 2871, 2306, 1716, 1703, 1456, 1368, and 1180 cm^{-1}.

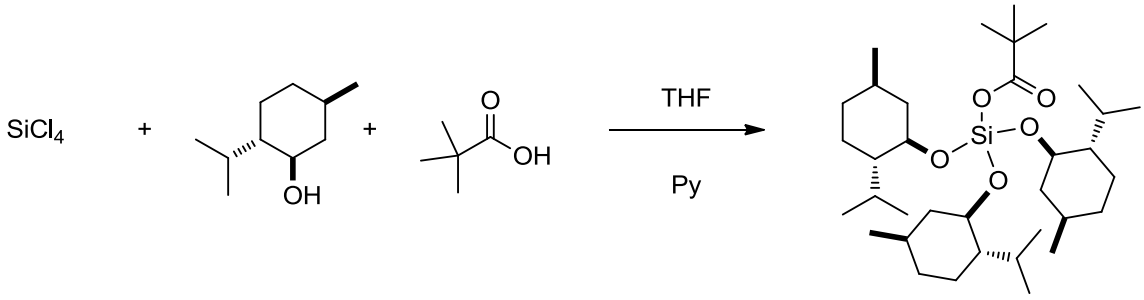

Pivalic (tris((1R,2S,5R)-2-isopropyl-5-methylcyclohexyl) orthosilicic) anhydride (*7*). THF (200 mL) was placed in a 250 mL round bottom flask, placed under a nitrogen atmosphere, and stirred. $SiCl_4$ (0.5 ml, 4.36 mmol) was added by glass syringe. Menthol (2.078 g, 13.3 mmol), pyridine (0.344 g, 13.3 mmol), and THF (20 mL) were combined and added dropwise to the $SiCl_4$ mixture. After 1 h pivalic acid (0.4457 g, 4.36 mmol) and pyridine (0.3441 g, 4.36 mmol) were added by syringe to the reaction mixture. The reaction was monitored by TLC (95:5, Hexanes: Ethyl Acetate). After 24 h the mixture was filtered, concentrated down, and purified by MPLC (99.5:0.5, Hexanes: Ethyl Acetate) to yield a clear colorless oil (82%). **^{1}H NMR** (500 MHz, C(O)D_6): δ 3.83 (dt, *J* = 10.8, 4.4 Hz, 3H, SiOC*H*), 2.28 (dsept, *J* = 2.5, 6.9 Hz, 3H, $(CH_3)_2$C*H*), 2.11 (m, 3H, SiOCHCH_A*H*$_E$), 1.64 (m, 6H, $(CH_3)_2$CHCHCH_A*H*$_E$CH_A*H*$_E$), 1.38 (m, 3H, CH_3C*H*),1.21 (s, 9H, (C*H*$_3$)$_3$), 1.17 (ddt, *J* = 12.5, 8.3, 11.2 Hz, 3H, $(CH_3)_2$CHC*H*), 1.04 (app. q, *J* = 11.8 Hz, 3H, $(CH_3)_2$CHCHC*H*$_A$H$_E$), 0.95 (m, 3H,

$(CH_3)_2CHCHCH_2CH_AH_E$), 0.90 (dd, *J* = 1.5, 6.9 Hz, 18H, $(CH_3)_2$), 0.86 (m, 3H, $SiOCHCH_AH_E$), and 0.79 (d, *J* = 6.9 Hz, 9H, CH_3); **^{13}C NMR:** (125 MHz, $CO(CD_3)_2$) 176.49, 80.25, 74.46, 49.46, 44.25, 34.35, 31.60, 25.24, 22.68, 22.14, 21.14, 15.71, and 14.68; ; **HR ESI-MS**: calcd for $C_{325}H_{66}NaO_5Si$ 617.4572[M + Na]$^+$, found 617.4593; **IR** (CH_2Cl_2): 2951, 2919, 2868, 1725, 1457, 1384, 1368, 1290, 1235, 1173, 1085, 1053, and 1002 cm^{-1}.

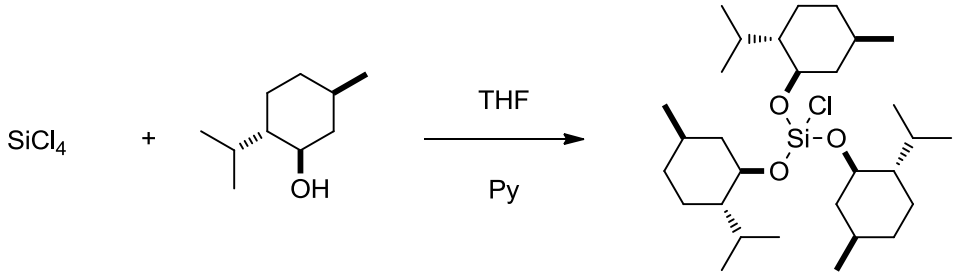

8

Chlorotris(((1R,2S,5R)-2-isopropyl-5-methylcyclohexyl)oxy)silane (*8*). THF (200 mL) was placed in a 250 mL round bottom flask, placed under a nitrogen atmosphere, and stirred. $SiCl_4$ (0.5 ml, 4.36 mmol) was added by glass syringe. Menthol (2.078 g, 13.3 mmol), pyridine (0.344 g, 13.3 mmol), and THF (20 mL) were combined and added dropwise to the $SiCl_4$ mixture. The reaction mixture was filtered, concentrated, and purified by MPLC (Hexanes: Ethyl Acetate, 99:1) to yield a clear colorless oil (72%). **^{1}H NMR** (500 MHz, $CDCl_3$): δ 3.70 (dt, *J* = 10.8, 4.4 Hz, 3H, SiOC*H*), 2.20 (dsept, *J* = 2.5, 7.4 Hz, 3H, $(CH_3)_2CH$), 2.07 (m, 3H, $SiOCHCH_AH_E$), 1.61 (m, 6H, $(CH_3)_2CHCHCH_AH_ECH_AH_E$), 1.37 (m, 3H, CH_3CH), 1.20 (ddt, *J* = 2.3, 9.8, 10.3 Hz, 3H, $(CH_3)_2CHCH$), 1.03 (q, *J* = 10.8 Hz, 3H, $(CH_3)_2CHCHCH_AH_E$), 0.95 (m, 3H, $(CH_3)_2CHCHCH_2CH_AH_E$), 0.90 (dd, *J* =

5.4, 6.9 Hz, 18H, (CH_3)$_2$), 0.87 (m, 3H, SiOCHCH_AH$_E$), and 0.77 (d, *J* = 7.3 Hz, 9H, CH_3); **^{13}C NMR:** (125 MHz, $CDCl_3$) 74.46, 49.46, 44.26, 34.35, 31.60, 25.24, 22.68, 21.14, 21.13,15.71 and 14.68; **HR ESI-MS**: calcd for $C_{30}H_{57}ClNaO_3Si$ 551.3658 $[M + Na]^+$, found 551.3684; **IR** (neat): 2956, 2927, 2870, 1456, 1385, 1369, 1237, 1180, 1085, 1053, 1003, and 553 cm^{-1}.

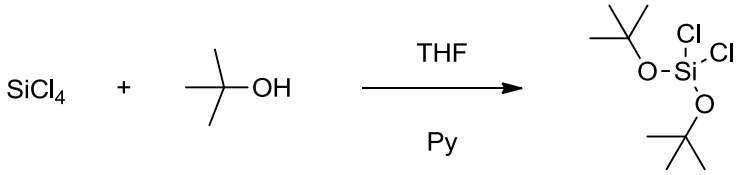

9

Di-tert-butoxydichlorosilane (*9*). THF (200 mL) was placed in a 250 mL round bottom flask, placed under a nitrogen atmosphere, and stirred. $SiCl_4$ (2.0 ml, 17.45 mmol) was added by glass syringe. *t*-Butanol (2.846 g, 38.41 mmol), pyridine (3.038 g, 38.41 mmol), and THF (20 mL) were combined and added dropwise to the $SiCl_4$ mixture. The reaction was allowed to stir 10 h before it was filtered, concentrated, and purified by distillation to yield a clear colorless oil (57%). **^{1}H NMR** (75 MHz, $CDCl_3$): δ 1.42 (s, 18 H); **^{13}C NMR:** (125 MHz, $CDCl_3$) 77.99 and 31.03; **HR ESI-MS**: calcd for $C_{10}H_{24}Na_1O_4Si_1$ 259.1336 $[(tBuO)_2Si(OMe)_2 + Na]^+$, found 259.1325; **IR** (neat): 2982, 1394, 1369, 1246, 1180, 1092, and 1071 cm^{-1}.

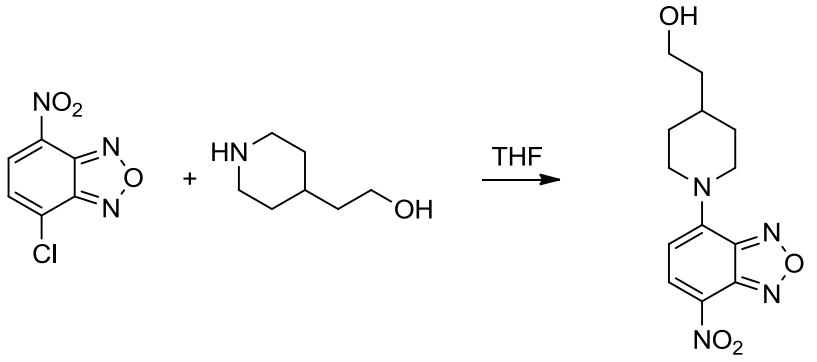

11

2-(1-(7-nitrobenzo[c][1,2,5]oxadiazol-4-yl)piperidin-4-yl)ethanol(*11*). 4-Chloronitrobenzooxadiazole (1 mmol, 200 mg) was dissolved in THF (30 mL) and brought to 0 °C. 4-Piperdine ethanol (2.01 mmol, 0.2603 g) was added dropwise to the solution and allowed to stir for 30 min. The reaction mixture was brought to room temperature and allowed to stir for 1h. A red precipitate was observed following the addition of the 4-piperdine ethanol and the completion of the reaction was monitored by TLC (100% EtOAc). The mixture was concentrated and passed through silica gel (2:1 Acetone:EtOAc) and concentrated. The reaction was recyrstallized (99:1 EtOAc:Hexanes) to yield a bright red solid in 80% yield. **^{1}H NMR** (500 MHz, $CDCl_3$) δ 8.44 (d, *J* = 8.8 Hz, 1H, $NO_2CC\mathit{H}$), 6.29 (d, *J* = 8.8 Hz, 1H, $NO_2CCHC\mathit{H}$), 4.86 (bd, *J* = 11.8 Hz, 2H, $NC\mathit{H}_{eq}H_{ax}$), 3.77 (t, *J* = 5.4 Hz, 2H, $C\mathit{H}_2OH$), 3.38 (dt, *J* = 2.0, 13.2 Hz, 2H, $NCH_{eq}\mathit{H}_{ax}$), 2.04 (m, 2H, $NCH_2CH_{eq}\mathit{H}_{ax}$), 1.99 (m, 1H, $C\mathit{H}CH_2CH_2OH$), 1.60 (q, *J* = 6.4 Hz, 2H, $C\mathit{H}_2CH_2OH$), and 1.46 (ddddd, *J* = 4.4, 11.7, 11.7, 11.7, 13.7 Hz, 2H, $NCH_2C\mathit{H}_{eq}H_{ax}$); **^{13}C NMR** (75 Hz, 300 MHz): 146.24, 146.18, 146.09,136.66, 103.66, 69.16, 59.82, 51.33, 39.90, 33.25, 33.17; **HR ESI-MS**: calcd for

$C_{13}H_{16}N_4NaO_4$ 315.1064[M + Na]$^+$, found 315.1076; **IR** (CH_2Cl_2): 3282(b), 2926, 1607, 1553, 1487, 1447, 1331, 1319, 1261, 1237, and 1088 cm^{-1}

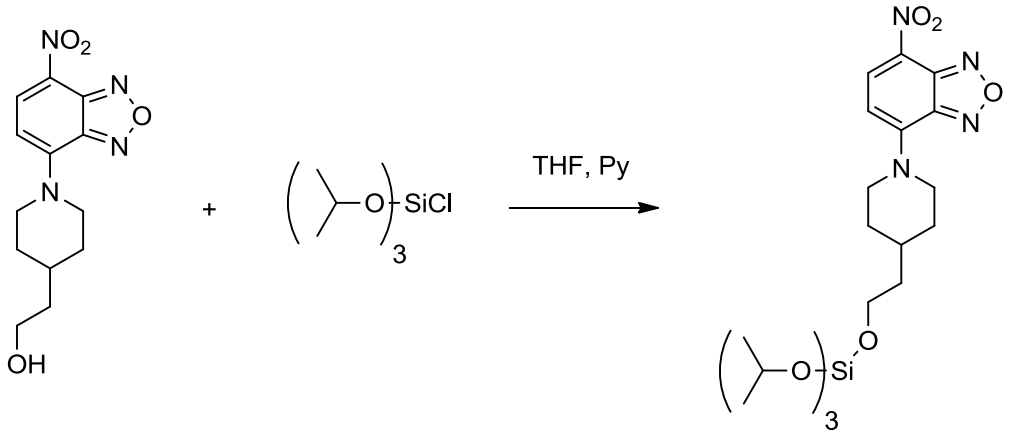

11 ***12***

Triisopropyl (2-(1-(7-nitrobenzo[c][1,2,5]oxadiazol-4-yl)piperidin-4-yl)ethyl) orthosilicate (*12*). Triispropylchlorosilane (0.14 mmol, 33 mg) was placed in a culture tube with dry THF (1 mL). Compound ***11*** and pyridine were dissolved in THF (1 mL). This solution was added dropwise to the silane mixture. The culture tube was then flushed with nitrogen and allowed to react for 4h. The resulting mixture was filtered through glass wool and concentrated to give a red solid. The crude product was purified by MPLC Column (4:1 Hexanes: Ethyl Acetate) to yield a bright red solid (70%). **^{1}H NMR** (500 MHz, $CDCl_3$) δ 8.44 (d, *J* = 9.3 Hz, 1H, $NO_2CC\mathit{H}$), 6.62 (d, *J* = 9.3 Hz, 1H, $NO_2CCHC\mathit{H}$), 4.94 (bd, *J* = 12.7 Hz, 2H, $NC\mathit{H}_{eq}H_{ax}$), 4.23 (sept., *J* = 5.85 Hz, 3H, $(CH_3)_2C\mathit{H}$), 3.87 (t, *J* = 6.4 Hz, 2H, $C\mathit{H}_2OH$), 3.38 (dt, *J* = 13.7, 2.5 Hz, 2H, $NCH_{eq}\mathit{H}_{ax}$), 2.05 (m, 2H, $NCH_2CH_{eq}\mathit{H}_{ax}$),

1.96 (app. s, 1H, C*H*CH_2CH_2OH), 1.59 (q, *J* = 6.4 Hz, 2H, C*H*$_2CH_2OH$), 1.46 (ddddd, *J* = 3.9, 11.7, 11.7, 11.7, 13.7 Hz, 2H, $NCH_2CH_{eq}H_{ax}$) and 1.19 (d, *J* = 6.4 Hz, 18H, $(CH_3)_2CH$) ; **^{13}C NMR** (75 Hz, $CO(CD_3)_2$): 146.30, 146.21, 146.18, 146.07, 103.69, 66.46, 61.27, 51.28, 39.22, 33.13, 33.09, and 25.77; **HR ESI-MS**: calcd for $C_{13}H_{16}N_4NaO_4$ 315.1064$[M + Na]^+$, found 315.1076; **IR** (CH_2Cl_2): 3055, 2976, 2936, 1612, 1547, 1294, 1173, 1136, 1117, and 1040 cm^{-1}

2. Amide Bond Formation Kinetics in the Selective Uptake of Aliphatic Amines in PEG-PLGA Block-Copolymer Nanoparticles

2.1 Background

Hydrophobic-hydrophillic AB diblock-copolymers have had an increasing interest in their use to form spherical micellar structures in aqueous media. These aqueous micellar systems are potentially useful for applications in the field of pharmacology, ecology, the painting and printing industry, and agriculture.[29] Their diversity of applications comes, in part, from their ability to uptake or release organic molecules into the surrounding aqueous environment. This ability gives them the potential to be utilized as delivery vehicles for hydrophobic drugs.

An estimated 40% of emerging drug candidates are hydrophobic in nature.[30] Not only do most of these compounds have low aqueous solubility, many also have unfavorable pharmacokinetics, poor biodistribution profiles, and toxicitiy issuses that prevent full utilization of their therapeutic potential.[31] Nanoparticles for hydrophobic drug delivery made from biodegradable polymers have the potential to provide advantages over other formulations for these drugs. These include longer stability in storage and in vivo, greater solubility for hydrophobic drugs, fewer side effects from surfactants in the formulation, and targeted delivery either through active or passive means.[32] With the possibility for these improvements on current drug formulations, it is necessary to get a complete understanding of these polymeric systems, including characteristics surrounding transfer of molecules through the polymer matrix.

For polymeric nanoparticles it is generally assumed that the higher the hydrophobic nature (log P) of the drug or molecule in question, the higher its preference to remain in the hydrophobic nanoparticle core. Vice-versa the more hydrophillic the molecule the more it will prefer to be in the aqueous media surrounding the polymeric nanoparticles.[33] While these generalizations are useful and widely accepted, frequently the preference of location of the compound in question is dependent on many factors; surface adsorption/desorption, diffusion through particle pores, diffusion through intact polymer, the volume of surrounding media, diffusion through water swollen polymer, surface or bulk erosion of polymer matrix, etc.[34]

Starting in the mid 1970s there has been an increased focus on utilizing organized media, such as micelles and nanoparticles, to perfom highly selective and fast chemical reactions, in particular to obtain the catalytic effects close to those observed within enzymes. Since then, considerable effort has been devoted to micellar catalysis of organic reactions but in general the results were not as great as expected.[35] With the extensive work performed on organic reactions in organized media there is still very little reference or insight describing the effect of selective uptake of reagents into the hydrophobic nanoparticle core based upon sterics or hydrophobicity. Better understanding of characteristics of selective uptake can lead to improved understanding and design of polymer nanoparticles for drug loading and drug delivery.

2.2 Studies

While working with the PEG-PLGA nanoparticles formed by FNP, as described in Part 1, the question arose as to what type of compounds would be selectively taken up into its hydrophobic core. To begin to probe this question we decided to design a chemical reaction that would have the potential to occur inside the nanoparticle. In order for a chemical reaction to provide insight into selective uptake, certain parameters would have to be met; i) the reaction has to be faster than the diffusion between the aqueous medium and the core, ii) the rate of mixing (complete distribution of reagents) has to be faster than the rate of reaction, and iii) the reaction should be bimolecular in nature where one of the reactants is held within the core, generally through a covalent bond or strong intermolecular interactions.

To find a chemical reaction that was fast and irreversible, we turned to an amide bond formation reaction between an ester and an aliphatic amine (Scheme 5). In this design altering R^1 or R^2 could change the hydrophobic and steric properties of the amine, giving us the potential to analyze effects of selective uptake. R^3 was devised to have a hydrophobic tail that would prefer to remain in the nanoparticle core, while X was aimed to be a good leaving group to make the reaction favorable and fast.

Scheme 5: Amide bond formation.

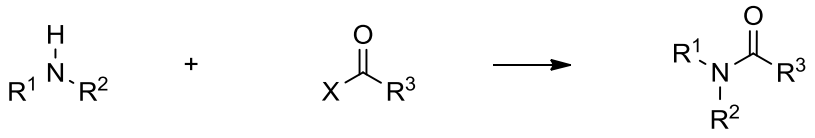

R^1,R^2 = H or alkyl X = Leaving Group
R^3 = Hydrophobic Tail

The leaving group, X, was selected to be 2,4-dinitrophenol for its excellent ability to act as a leaving group, a way to visibly monitor reaction completion by the formation of a bright yellow color when the 2,4-dinitrophenol anion is released, and for the simplicity and diagonstic aspects of its ^{1}H NMR spectrum. The hydrophobic tail, R^3, was set as an oleyol carbon chain because it has a long greasy tail that would favor the hydrophobic nanoparticle core, a cis double bond present to give us a handle in its ^{1}H NMR spectrum, it is easy to synthetically manipulate, and it is cost effective. Steroidal compounds were considered when designing the ester in order to more closely mimic hydrophobic drugs. However, these were either not cost effective or they contained other functional groups that had the potential to interfere with the study. It is an assumption that the intermolecular interactions are sufficiently strong that the greasy oleic ester will stay in the hydrophobic core. To make ester ***13*** 2,4-dinitrophenol was coupled with oleic acid using dicyclohexyl carbodiimide (DCC) in methylene chloride (Scheme 6).

Scheme 6: Formation of hydrophobic ester, ***13***.

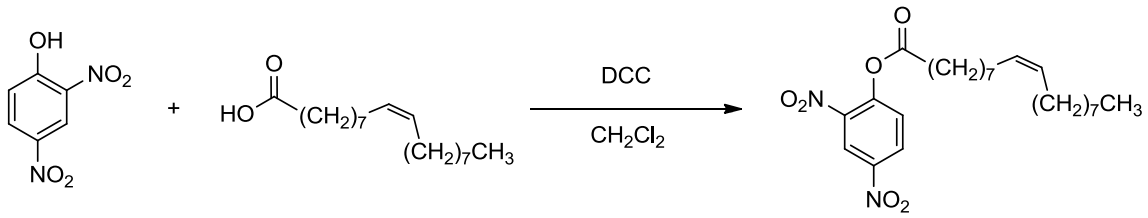

13

In planning which types of amines to compete in order to form the amide bond there are certain limitations that have to be considered. First, the amines have to be completely soluble in the 95:5 water:THF mixture outside of the nanoparticles in a ten molar equivalent excess in comparison to the ester. Second, the amines have to be close enough in reaction rate to get measurable data by ^{1}H NMR spectroscopy so that appropriate conclusions can be drawn. For this purpose a variety of aliphatic amines were competed in a homogeneous chloroform solution from which four amines were chosen for the nanoparticle competition experiments; *n*- hexylamine, diethylamine, dipentylamine, and dimethylamine (Figure 9).

Figure 9: Amines chosen for competition experiments.

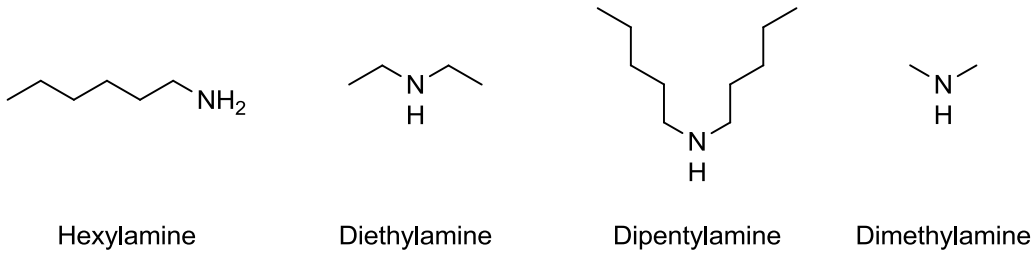

The physical design of the experiment was as follows; the nanoparticles were formed using FNP where the hydrophic ester was dissolved in the THF with the polymer before impingement jet mixing. The newly formed solution of nanoparticles was placed in an ice bath to slow the rate of reaction, and a stock solution of two competitive amines dissolved in THF were added to the cooled solution and stirred for 30 minutes. The products were extracted with methylene chloride and analyzed by ^{1}H NMR spectroscopy to obtain the ratio of amide

products. The competition reactions were also performed in deuterated chloroform, where ten equivalents of a stock solution of two competitive amines was added to the ester at zero degrees Celsius, and the amide product ratios were analyzed by ^{1}H NMR spectroscopy.

The observed rate constants for the competition of the amines were determined through ^{1}H NMR analysis from the product ratio of the two amides that were formed. The product ratio reflects the relative rate constants of the two amines as long as the concentration of the amines in the competition is held constant (Scheme 7). In order to do this each amine was used in a ten molar equivalent excess in comparison to the starting hydrophobic ester.

Scheme 7: Kinetics of competitive amide bond formation.

$$\text{Amine}^1 + \text{Amine}^2 + \text{Ester} \longrightarrow \text{Amide}^1 + \text{Amide}^2$$

$$-\frac{d[\text{Amide}^1]}{dt} = k_1[\text{Amine}^1][\text{Ester}]$$

$$-\frac{d[\text{Amide}^2]}{dt} = k_2[\text{Amine}^2][\text{Ester}]$$

divide the equations and set amines as constants $\Longrightarrow$ $\frac{[\text{Amide}^1]}{[\text{Amide}^2]} = \frac{k_1}{k_2}$

The results from the amide competitions in deuterated chloroform (Table 2) follow with expected stereoelectronic effects of amines, in this case nucleophilicity.[36] Hexylamine is faster than both diethylamine and dipentylamine mainly due to steric effects. However, both the dipentylamine and the diethylamine are competitive because they have a higher electron density from

the extra carbon chain making the nitrogen atom more nucleophilic. Diethylamine and dimethylamine are both faster than dipentylamine; again steric effects appear to be the overriding factor since all of them are dialkylamines.

Table 2: Results from amide competitions in chloroform and PEG-PLGA nanoparticles.

	A : B	A : C	B : C	D : C
Chloroform	1 : 0.23	1 : 0.21	1 : 0.72	>99 : 1
Nanoparticles	>99 : 1	1 : 0.12	1 : 1.39	1 : 0.11

* the largest error for any of the ratios is ± 0.05

A = Hexylamine
B = Diethylamine
C = Dipentylamine
D = Dimethylamine

The high preference of the hexylamine over the diethylamine in the nanoparticle solution was a unexpected result. In general we would have expected to see the more hydrophobic amines selectively diffusing into the nanoparticle and reacting first. While it can be argued that the hexylamine is more hydrophobic than the diethylamine, the fact that none of the diethylamine could be detected by ^{1}H NMR analysis was surprising in light of the fact that the diethylamine was competitive when compared to dipentylamine.

A possible explanation for the the high selectivity of hexylamine uptake into the nanoparticles may be attributed to the entropy and enthalpy required for the amines to diffuse through the polymer matrix, particularly in consideration with the higher degree of self-association of primary amines. There has been

little literature precedence examining the self-association of free base amines in water, particularly those of low molecular weight. However there is a plethora of work pertaining to the salts of alkylamines describing amphiphilic properties such as self-association in polar solvents and accumulation at colloidal interfaces.[37] Studies have shown that octylamine, which forms a crystalline hydrate in water, tends to aggregate as the system cools and shows indication of micellar behavior.[38,39] Primary and seconardy amines are known to self-associate in alkanes due to observed deviations from Raoult's law, making them non-ideal solutions.[40] As for neutral primary amines previous work has shown self-association through IR spectroscopy, but again no work has been done to show the degree to which primary amines may self-associate over secondary amines.[41] In terms of theoretical work that has been completed, primary amines are said to self-associate more than secondary and tertiary amines in polar *n*-alcohol solvents, such as propanol, due to their ability to form strong hydrogen bonds.[42,43]

If we assume self-association is stronger for hexylamine than for dialkylamines, hexylamine would have a lower entropic barrier to enter the nanoparticle core because its degrees of freedom are already limited due to its self-association. This high entropic preference, along with the fact that it is more hydrophobic (log P of 2.08 for hexylamine and 0.50 for diethylamine, calculated from ACD labs software), may explain the high selectivity for hexylamine to diffuse into the nanoparticle core.

The dipentylamine would be enthalpically favored over hexylamine due to its high degree of hydrophobicity, (Log P of 3.42, ACD Labs). However, the hexylamine still shows a high degree of selectivity which may be explained by its ability to self-associate.

The competitve reaction of dipentylamine and diethylamine follows what we would have expected a preference for the dipentylamine to be selectively taken up into the nanoparticle core due to its higher hydrophobicity. The result is significant but the formation of the dipentylamide is not overwhelmingly favored, potentially due to the higher entropic barrier of dipentylamine diffusing into the core over diethylamine.

The last reaction, the competition of dipentylamine and dimethylamine, was chosen because we wanted to analyze the two extremes that we could achieve for any one pair of our water-soluble amines. The presence of dipentylamide in a 1 to 10 ratio with dimethylamide is a promising result but there is no way to judge by our methods the extent to which dimethylamide was favored in the chloroform competition, which leads to the inability to make an accurate quantitative comparison between the chloroform and nanoparticle competitions. The appearance of the dipentylamide in the nanoparticle solution does point to the generalization that the more hydrophobic amine will preferentially diffuse into the core, but further testing is needed.

2.3 Conclusion

A competitive amide bond formation reaction was designed to study the selective uptake into a PEG-PLGA nanoparticle formed by FNP. For this reaction two water soluble amines were competed in chloroform and in a nanoparticle suspension and the two ratios of the product amides were compared. In chloroform the results fall in line with what would be expected for the stereoelectronic effects for each of the amines to form the amide bond. For the competition reactions in the nanoparticle solution a surprising result was observed: a very high selectivity favoring hexylamine over diethylamine. It can be hypothesized that the hexylamine could self-associate, which would give it a higher preference to move into the hydrophobic core; more experimentation would have to be done to test this hypothesis.

2.4 Experimental

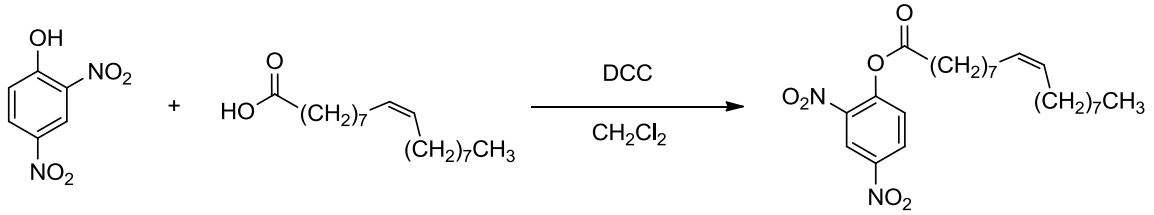

13

2,4-Dinitrophenyl Oleate (*13*). 2,4-Dinitrophenol (359 mg, 2.0 mmol) was dissolved in CH_2Cl_2 (40 mL) and added to a 50 mL culture tube. *N,N*-Dicyclohexylcarbodiimide (422 mg, 2.0 mmol) was added to the methylene chloride solution, followed by oleic acid (558 mg, 2.0 mmol). The reaction mixture was stirred for 1 h and then washed with sat. NH_4Cl (4 x 20 mL) and brine (1 x 20

mL), dried ($MgSO_4$), filtered, concentrated, and purified by MPLC (Hexanes:Ethyl Acetate, 90:10) to yield a clear pale yellow oil (83%). **^{1}H NMR** (500 MHz, $CDCl_3$) δ 8.96 (d, *J* = 2.9 Hz, 1H, $NO_2CCHCNO_2$), 8.51 (dd, *J* = 3.0, 8.8 Hz, 1H, NO_2CHCH), 7.46 (d, *J* = 8.8 Hz, 1H, NO_2CHCH), 5.35 (m, 2H, $CH_2CH{=}CHCH_2$), 2.69 (t, *J* = 7.4 Hz, 2H, $COCH_2$), 2.02 (m, 4H, $CH_2CH{=}CHCH_2$), 1.78 (p, *J* = 7.8 Hz, 2H, $COCH_2CH_2$), 1.31 (m, 20H, $(CH_2)_4CH_2C{=}CCH_2(CH_2)_6CH_3$) and 0.88 (t, *J* = 6.6 Hz, 3H, CH_3); **^{13}C NMR** (75 Hz, $CDCl_3$) 170.42, 133.47,130.06, 129.65, 128.93, 126.64, 121.69, 33.96, 31.88, 29.75, 29.64, 29.51, 29.31, 29.08, 29.03, 28.93, 27.21, 27.13, 24.27, 22.67, and 14.11; **IR** (neat): 3112, 3005, 2926, 2854, 1783, 1611, 1543, 1481, 1346, 1225, and 1079 cm^{-1}.

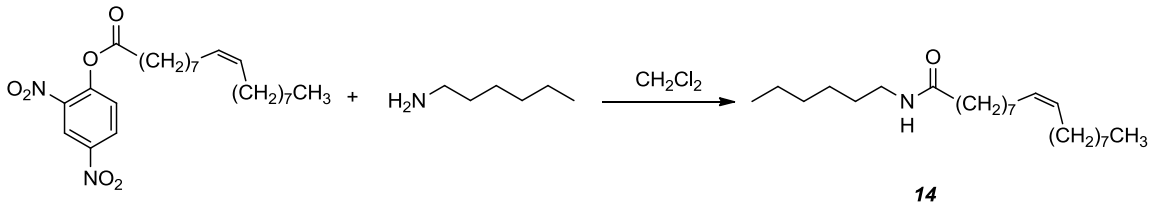

14

***N*-Hexyloleamide (*14*).** 2,4-Dinitrophenyl oleate (20 mg, 0.04 mmol) was placed in a culture tube with 10 mL of CH_2Cl_2 and set stirring. Hexylamine (4.5 mg, 0.04 mmol) was added dropwise to the solution and allowed to stir for 30 min. Upon addition of the amine a bright yellow color formed. The solution was concentrated and passed through silica gel (Hexanes:Ethyl Acetate 95:5), which yielded a clear colorless oil (94%). **^{1}H NMR** (500 MHz, $CDCl_3$) δ 5.34 (m, 2H, $CH_2CH{=}CHCH_2$), 3.23 (dt *J* = 5.9, 7.3 Hz, 2H, NCH_2), 2.15 (t, *J* = 7.4 Hz, 2H, $COCH_2$), 2.01 (m, 4H, $CH_2CH{=}CHCH_2$), 1.62 (p, *J* = 7.4 Hz, 2H, $COCH_2CH_2$), 1.49 (p, *J* = 7.8 Hz, 4H, NCH_2CH_2), 1.30 (m, 20H, $(CH_2)_4CH_2C{=}CCH_2(CH_2)_6CH_3$),

1.27 (m, 6H, $NCH_2CH_2CH_2CH_2CH_2$), 0.88 (t, *J* = 6.9 Hz, 6H, $N(CH_2)_4CH_3$), and 0.88 (t, *J* = 6.9 Hz, 3H, CH_3); **^{13}C NMR** (75 Hz, $CDCl_3$): 170.14, 135.60, 132.31, 39.48, 36.84, 31.83, 29.70, 29.64, 29.51, 29.09, 27.16, 27.11, 26.53, 25.81, 22.62, 14.07, and 13.94; **HR ESI-MS**: calcd for $C_{24}H_{47}NNaO$ 388.3550$[M + Na]^+$, found 388.3550; **IR** (neat): 2959, 2922, 2850, 1648, 1468, 1420, and 1381 cm^{-1}

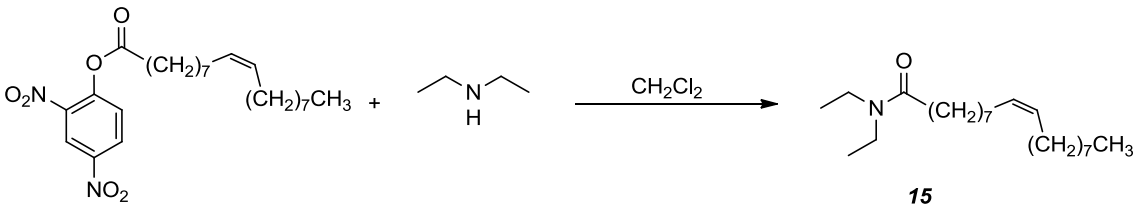

15

***N,N*-Diethyloleamide (*15*)**. 2,4-Dinitrophenyl oleate (20 mg, 0.04 mmol) was placed in a culture tube with 10 mL of CH_2Cl_2 and set stirring. Diethylamine (3.3 mg, 0.04 mmol) was added dropwise to the solution and allowed to stir for 30 min. Upon addition of the amine a bright yellow color formed. The solution was concentrated and passed through silica gel (Hexanes:Ethyl Acetate 9:1), which yielded a clear colorless oil (98%). **^{1}H NMR** (300 MHz, $CDCl_3$) δ 5.34 (m, 2H, CH_2CH=$CHCH_2$),3.37 (q, *J* = 7.3 Hz, 2H, NCH_2), 3.30 (q, *J* = 7.4 Hz, 2H, NCH_2), 2.28 (t, *J* = 7.4 Hz, 2H, $COCH_2$), 2.00 (m, 4H, CH_2CH=$CHCH_2$), 1.64 (p, *J* = 6.9 Hz, 2H, $COCH_2CH_2$), 1.29 (m, 20H, $(CH_2)_4CH_2C$=$CCH_2(CH_2)_6CH_3$), 1.17 (t, *J* = 6.9 Hz, 3H, NCH_2CH_3), 1.11 (t, *J* = 6.9 Hz, 3H, NCH_2CH_3), and 0.88 (t, *J* = 6.8 Hz, 3H, CH_3); **^{13}C NMR** (75 Hz, $CDCl_3$): 129.91, 129.77, 41.91, 39.97, 33.15, 31.87, 29.74, 29.71, 29.62 29.50, 29.30, 27.18, 25.58, 25.48, 22.66, 14.38,

14.10, and 13.09 ; **HR ESI-MS**: calcd for $C_{22}H_{43}NNaO$ 360.3237[M + Na]$^+$, found 360.3231; **IR** (neat): 2924, 2853, 1642, 1461, 1428, 1378, and 1364 cm^{-1}.

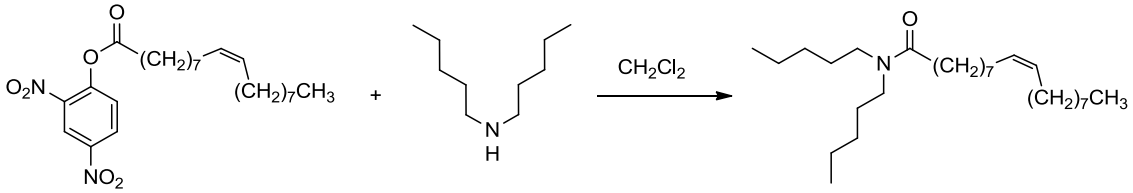

17

***N,N*-Dipentyloleamide (*16*).** 2,4-Dinitrophenyl oleate (20 mg, 0.04 mmol) was placed in a culture tube with 10 mL of CH_2Cl_2 and set stirring. Dipentylamine (7.0 mg, 0.04 mmol) was added dropwise to the solution and allowed to stir for 30 min. Upon addition of the amine a bright yellow color formed. The solution was concentrated and passed through silica gel (Hexanes:Ethyl Acetate 95:5), which yielded a clear colorless oil (95%). **^{1}H NMR** (300 MHz, $CDCl_3$) δ 5.34 (m, 2H, CH_2CH=$CH$$CH_2$), 3.28 (t, *J* = 7.7 Hz, 2H, NCH_2), 3.20 (t, *J* = 7.7 Hz, 2H, NCH_2), 2.28 (t, *J* = 7.3 Hz, 2H, $COCH_2$), 2.00 (m, 4H, CH_2CH=$CHCH_2$), 1.61 (p, *J* = 7.7 Hz, 2H, $COCH_2CH_2$), 1.51 (m, 4H, NCH_2CH_2), 1.30 (m, 20H, $(CH_2)_4CH_2C$=$CCH_2(CH_2)_6CH_3$), 1.28 (m, 8H, $NCH_2CH_2CH_2CH_2$), 0.92 (t, *J* = 6.9 Hz, 6H, $N(CH_2)_4CH_3$), and 0.88 (t, *J* = 6.9 Hz, 3H, CH_3); **^{13}C NMR** (75 Hz, $CDCl_3$): 129.92, 129.79, 47.92, 45.78, 33.15, 31.88, 29.73, 29.69, 29.64, 29.51, 29.40, 29.31, 29.20, 29.03, 28.83, 27.46, 27.18, 25.52, 22.67, 22.49, 22.44,

14.11, 14.05, and 14.00; **HR ESI-MS**: calcd for $C_{28}H_{55}NNaO$ 444.4176[M + Na]$^+$, found 444.4197; **IR** (neat): 2955, 2924, 2854, 1648, 1461, 1422, and 1377 cm^{-1}.

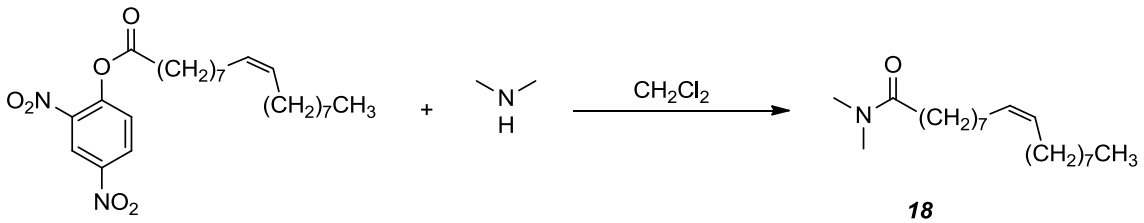

18

***N,N*-Dimethyloleamide (*17*).** 2,4-Dinitrophenyl oleate (20 mg, 0.04 mmol) was placed in a culture tube with 10 mL of CH_2Cl_2 and set stirring. Dimethylamine was bubbled into the solution until a persistent yellow color was formed. The reaction mixture was concentrated and passed through silica gel (Hexanes:Ethyl Acetate 9:1), which yielded a clear colorless oil (70%).**^{1}H NMR** (300 MHz, $CDCl_3$) δ 5.35 (m, 2H, CH_2CH=$CH$$CH_2$), 3.01 (s, 3H, NCH_3), 2.94 (s, 2H, NCH_3), 2.30 (t, *J* = 7.8 Hz, 2H, $COCH_2$), 2.02 (m, 4H, CH_2CH=$CHCH_2$), 1.63 (p, *J* = 7.4 Hz, 2H, $COCH_2CH_2$), 1.30 (m, 20H, $(CH_2)_4CH_2C$=$CCH_2(CH_2)_6CH_3$), and 0.88 (t, *J* = 6.9 Hz, 3H, CH_3); **^{13}C NMR** (75 Hz, $CDCl_3$): 130.05, 129.63, 37.27, 35.33, 31.88, 29.74, 29.71, 29.62, 29.50, 29.30, 29.0729, 29.02, 27.20, 25.16, 24.27, 22.67, 14.10 ; **HR ESI-MS**: calcd for $C_{20}H_{39}NNaO$ 332.2924[M + Na]$^+$, found 332.2936; **IR** (neat): 2924, 2853, 1738, 1648, 1537, 1463, 1397, and 1344 cm^{-1}.

References

[1] U.S. Food and Drug Administration. *TAXOL® (paclitaxel) INJECTION*. **2007**. The package insert for the Bristol Meyers Squibb product: http://packageinserts.bms.com/pi/pi_taxol.pdf (last accessed August 1, 2011).

[2] Yokoyama, M. *Polymeric Drug Delivery I*, Chapter 3**, 2006**, pp 27-39, *ACS Symposium Series*, Volume 923

[3] Momparler, R. L.; Karon, M.; Siegel, S. E.; Avila, F. *Cancer Research* **1976**, *36*, 2891-2895.

[4] Shenoy, D. B.; Amiji, M. M. *Int. J. Pharm.* **2005**, *293*, 261-270.

[5] Safra, T. *Ann. Oncol.* **2000**, 1029-1033.

[6] Schroeder, U. *J. Pharm. Sci.* **1998**,1305-1307.

[7] Raghuvanshi, R. S. *Int. J. Pharm.* **2002**, 109-121.

[8] Iyer, A. K.; Khaled, G.; Fang, J.; Maeda, H. *Drug Discov. Today* **2006***, 11,* 812-818*.*

[9] Peppas, L.; Blanchette, J. O. *Adv. Drug Delivery Rev*. **2004**, *56*, 1649-1659.

[10] Maeda, H.; Sawa, T.; Konno, T. *J. Control. Rel.* **2001**, *74*, 47-61.

[11] (a) Johnson, B. K. Ph. D. Dissertation, Princeton University **2003**. (b) Johnson, B. K.; Prud'homme, R. K. U.S. PPA 2004/0091546 A1. (c) Johnson, B. K.; Prud'homme, R. K. *AIChE J.* **2003**, *49*, 2264-2282.

[12] Saad, W.S. Ph. D. Dissertation, Princeton University, Princeton, NJ, **2007**.

[13] Zhengxi Zhu, Ph. D. Dissertation, University of Minnesota, **2010**.

[14] Ansell, S. M.; Johnstone, S. A.; Tardi, P. G.; Lo, L.; Xie, S.; Shu, Y.; Harasym, T. O.; Harasym, N. L.; Williams, L.; Bermudes, D.; Liboiron, B. D.; Saad, W.; Prud'homme, R. K.; Mayer, L. D. *J. Med. Chem*. **2008**, *51*, 3288-3296.

[15] Forrest, M. L.; Yáñez, J. A.; Remsberg, C. M.; Ohgami, Y.; Kwon, G. S.; Davies, N. M. *Pharm. Res.* **2007**, *25*, 194-206.

[16] Turner, C. W.; Franklin, K. J. *J. Non-Cryst. Solids* **1986**, *91*, 402-415.

[17] Ro, J. C.; Chung, I. J. *Non-Cryst. Solids* **1989**, *110*, 26-32.

[18] Zerda, T. W.; Hoang, G. *Chem. Mater.* **1990**, *2*, 372-376.

[19] (a) Martin, K. R. *J. Nutr. Health Aging* **2007**, *11*, 94-97. (b) Iler, R. K. *The Chemistry of Silica: Solubility, Polymerization, Colloid and Surface Properties and Biochemistry of Silica*; John Wiley & Sons: Hoboken, NJ, **1979**.

[20] Gerrard, W.; Woodhead, A. H. *J. Chem. Soc*. **1951**, 519-522.

[21] **Patent:** US2566957 , **1951** ; C.A., **1952**, 3069.

[22] Beckmann, J. *J. of Organometallic Chem.* 648, **2002**, 188-192.

[23] Sauer, M; Meier, W. *Carrier-Base Drug Delivery*, Chapter 16, **2004**, *897*, 224-237, ACS Symposium Series.

[24] Yoo, H. S.; Park, T. G. *J. of Contr. Rel.* **2001**, *70*, 63-70.

[25] Danhier, F.; Lecouturier, N.; Vroman, B.; Jerome, C.; Marchand-Bryanert, J.; Feron, O.; Preat, V. *J. of Contr. Rel.* **2009**, *1*, 11-17.
[26] *Polarity of Solvents*.University of Rochester Chemistry Department *www.chem.rochester.edu/~nvd/**PolarityofSolvents**.doc*
[27] Herman, B.; Lakowicz, J. R.; Johnson, I. D.; Davidson, M. W. *Solvent Effects on Fluorescence Emission* **2010**, Olympus America Inc. http://www.olympusmicro.com/primer/java/jablonski/solventeffects/index.html
[28] Wong, J. E.; Duchscherer, T. M.; Pieatraru, G.; Cramb, D. T.; *Langmuir,* **1999**, *15*, 6181-6186.
[29] Sauer, M.; Meier, W. *Carrier-Based Drug Delivery*, Chapter 16, **2004,** *ACS Symposium Series*, 224-237.
[30] Hite, M.; Turner, S.; Federici, C. Part 1: Oral Delivery of Poorly Soluble Drugs. *Pharmaceutical Manufacturing and Packing Sourcer* **2003**.
[31] De Villiers, M. M.; Aramwit, P.; Kwon, G. S. Nanotechnology in Drug Delivery, **2009**, American Association of Pharmaceutical Sciences.
[32] Barratt, G. *Cell. Mol. Life Sci*. **2003**, 21-37.
[33] Petersen, S.; Fahr, A.; Bunjes, H. *Mol. Pharm*. **2010**, *2*, 350-363.
[34] Polakovic, M.; Gorner, T.; Gref, R.; and Dellacherie, E. *J. of Contr. Rel.* **1999**, 169-177.
[35] Ruasse, M. F.; Blagoeva, I. B.; Ciri, R.; Garcia-Rio, L.; Leis, J. R.; Marques, A.; Mejuto, J.; Monnier, E. *Pure and Appl. Chem*. **1997**, *9*, 1923-1932.
[36] Brotzel, F.; Cheng Chu, Y.; Mayr, H. *J. Org. Chem*. **2007**, *72*, 3679-3688.
[37] Backlund, S.; Friman, R.; Karlsson, S. *Colloids Surfaces A: Physicochem. Eng. Aspects* **1997**, *123-124*, 125-133.
[38] Ralston, A. W.; Hoerr, C.; Hoffman, E. J. *JACS* **1942**, 1516.
[39] Friberg, S.; Mandell, C. *J. Pharm. Sci*. **1970**, *59*, 1001.
[40] Kaarsholm, M.; Derawi, S.; Michelsen, M.; Kontogeorgis, G. *Ind. Eng. Chem. Res.* **2005**, *44*, 4406-4413.
[41] Wolff, H.; Schmidt, U.; Wolff, E. *Spectrochimica Acta Part A: Mol. Spec.* **1980,**. *10,* 899-901.
[42] Gonzales, J. A.; de la Fuenta, I. G.; Cobos, J. C. *Fluid Phase Equil*. **2000**, *168*, 31-58.
[43] Oswal, S. L. *Thermochimica Acta* **2005**, *1-2*, 59-68.